

Optimal Design of an Enclosure for a Portable Generator

by
Joseph E. Blanks

Thesis submitted to the faculty of the
Virginia Polytechnic Institute and State University
in partial fulfillment of the requirements for the degree of
Masters of Science

in
Mechanical Engineering

APPROVED:

William R. Saunders, Chairman
Harry H. Robertshaw
Douglas J. Nelson

February 7, 1997
Blacksburg, Virginia

KEY WORDS: Close fitting enclosure, Acoustic Enclosure, Acoustic Isolation,
Insertion loss, Passive acoustical treatment, optimization

Optimal Design of an Enclosure for a Portable Generator

by
Joseph E. Blanks

William R. Saunders, Committee Chairman

Department of Mechanical Engineering

Abstract

A simple, effective design for enclosing portable generators to reduce the radiated noise is an idea that seems to be desired by the consumers in this market. This investigation is to determine the feasibility of producing such an enclosure for a generator.

Several engineering aspects are incorporated in the design of the enclosure. The first, and probably the most paramount, are the acoustical effects of the enclosure itself. The investigation follows the theories for insertion loss of a close fitting enclosure. The thesis examines the system behavior of a close fitting enclosure that most acoustic text books ignore and how the material stiffness, density and source-to-enclosure distance affect the insertion loss and effectiveness of the enclosure. Measured and theoretical sound pressure level around the generator before and after the application of the enclosure are presented using standards described by ISO standard 1344.

The second important consideration for the enclosure design involves the heat transfer characteristics. The requirements of cooling air to the generator are discussed. Also presented are some acoustic design considerations to prevent any “direct line of sight” to any of the necessary openings which will help in the overall insertion loss.

The use of an optimal engineering design technique is presented, demonstrating its strengths and weakness in this application. The optimization method used for the study is the Hooke and Jeeves, or pattern search method. This method solved for the optimum material properties in approximately 30 iterations depending on the initial starting points and the desired weighting parameters.

KEY WORDS: Close fitting enclosure, Acoustic enclosure, Acoustic isolation, Insertion loss, Passive acoustical treatment, Optimization

Acknowledgments

I would first like to thank my parents for their endless love and support. Also, thanks to Dr. Saunders and Dr. Robertshaw for offering me the opportunity to return to school and pursue a masters degree. I would also like to thank all the members of my committee for their guidance on this project. And thanks to all the new friends I made for making it fun!

Table of Contents	page
Abstract.....	ii
Acknowledgments.....	iii
Table of Contents.....	iv
Nomenclature.....	v
List of Figures.....	vi
List of Tables.....	vii
1 Introduction.....	1
1.1 Motivation -- The Need for a Generator Enclosure.....	2
1.2 Chapter Review.....	2
2 Literature Review	4
2.1 A Review of Sound Transmission Theories.....	4
2.1.1 Transmission Loss Prediction.....	5
2.2 A Review of Insertion Loss.....	11
2.2.1 A Text Book, Close Fitting Enclosure Model.....	11
2.3 Acoustic Absorbing Materials and Perforated Panels.....	13
3 Developing the Insertion Loss Model.....	15
3.1 A Practical Insertion Loss Model.....	15
3.1.1 Test Apparatus to Compare the Model to Test Data.....	18
3.1.2 Measured Insertion Loss Values.....	19
3.2 Constraints on The Model.....	20
3.3 Effects of Material Properties and Panel Dimensions on the Model.....	24
3.4 Test Comparison of a Prototype Enclosure with the Generator to the Insertion Loss Model.....	27
4 Design Methodology.....	30
4.1 Development of Pattern Search Optimization Code.....	31
4.1.1 Performance Index: Considerations and Sensitivity.....	33
4.1.2 Weighting of Parameters -- Cost, Insertion Loss, Weight.....	34
4.1.3 Results of the Optimization Code.....	35
4.2 Heat Transfer Model.....	36
4.3 Intake and Exhaust Considerations.....	39
5 Results and Conclusions.....	40
5.1 Future work and considerations.....	41
Appendix I ISO Calculation of Sound Power Level for Test Generator.....	44
Appendix II Optimization Code.....	49
Bibliography.....	75
Vita.....	77

Nomenclature

f	frequency [Hz]
ω	frequency [radians/ sec]
z	material impedance $[\text{Kg} / \text{m}^2\text{s}]$
P_x	amplitude of the pressure wave $[\text{N}/\text{m}^2]$
p_x	complex notation of the pressure wave $[\text{N}/\text{m}^2]$
u	pressure wave normal velocity [m/s]
k	acoustic wave number [radians/m]
d	distance from the source to the panel [m]
a	length of the panel [m]
b	width of the panel [m]
$\rho_0 c$	acoustic impedance $[\text{Kg} / \text{m}^2\text{s}]$
ρ	density of the panel $[\text{Kg} / \text{m}^3]$
η	damping coefficient of the material []
h	thickness of the panel [m]
S	panel surface area $[\text{m}^2]$
ν	Poisson's ratio [unitless]
B	bulk modulus of the material $[\text{N}^*\text{m}]$
τ	transmission loss coefficient []
TL	transmission loss [dB]
IL	insertion loss [dB]

List of Figures

page

Figure 2.1: Pressure Waves Normally Incident on a Panel.....	4
Figure 2.2: Predicted Transmission Loss of a Single Partition.....	8
Figure 2.3: Pressure Waves Normally Incident on a Double Panel.....	9
Figure 2.4: Predicted Transmission Loss of a Double Panel.....	10
Figure 3.1: Predicted Insertion Loss for Clamped and Simply Supported Models.....	18
Figure 3.2: Test box speaker orientation.....	19
Figure 3.3: Predicted vs. Actual Insertion Loss for Clamped Boundary Conditions....	19
Figure 3.4: Plot of Insertion Loss Nulls: Predicted vs. Insertion Loss Model.....	21
Figure 3.5: Predicted SPL, Calculated from the Insertion Loss Model Using a Noise SPL Spectrum.....	22
Figure 3.6: Constrained Insertion Loss Model Nulls.....	23
Figure 3.7: Effects on Insertion loss Due to Changes in Panel Dimensions.....	24
Figure 3.8: Effects on Insertion Loss Due to Changes in Source-to-Panel Distance....	25
Figure 3.9: Effects on Insertion Loss Due to Changes in Panel Thickness.....	26
Figure 3.10: Intake and exhaust openings on the test enclosure.....	26
Figure 3.11: Effects on Insertion Loss Due to Changes in Panel Density.....	27
Figure 3.12: Measured A weighted, Sound Pressure Level of the Generator in the Lab	28
Figure 3.13: A-Weighted SPL of the Generator With and Without the Enclosure.....	28
Figure 3.14: Actual and Predicted Insertion loss for the Prototype Enclosure.....	29
Figure 4.1: Example of a Pattern Search Method.....	30
Figure 4.2: Optimization GUI.....	32
Figure 4.3: Calculated Performance Index for Iterations of the Optimization Code....	34
Figure 4.4: Calculated Overall SPL for Iterations of the Optimization Code.....	35
Figure 4.5: Actual SPL vs. Predicted SPL Calculated Using the Optimization Code..	36
Figure 4.6: Generator Components and Component Location.....	37
Figure 4.7: Operating Cylinder Temperature Free Field Environment.....	37
Figure 4.8: Enclosure Energy Balance Diagram.....	38
Figure A1: Dimensions of the Generator.....	44
Figure A2: Test Measurement Surface.....	45
Figure A3: Measured Generator Sound Pressure Level.....	46
Figure A4: Measured Generator Sound Power Level in 1/3 Octaves Band.....	47
Figure A5: Measured Loudness of the Generator.....	48

List of Tables

page

Table A1: X, Y, Z coordinates of test surface..... 45

Chapter 1

Introduction

Noise is a hazard that we expose ourselves to every day without consideration. It can cause physical problems such as permanent hearing loss, as well as psychological traumas, like stress. More and more requirements by regulating bodies, like OSHA, are being applied to every facet of daily life in order to reduce noise pollution. Cars have limiting noise requirements; human exposure to noise in the work place is federally regulated; new buildings have code requirements on the amount of transmitted noise through its walls. There are two general methods which can be used to achieve the required noise levels; active and passive noise control.

Active noise control (ANC) is specific in its application. It works well for the control of low frequency noise sources. ANC requires state-of-the-art electronic hardware and precise computer software. Today it remains one of the more expensive forms of noise control, often requiring large amounts of engineering time and costly control systems.

The most cost effective and widely used form of noise suppression is still passive noise control. Passive control is achieved by the use of barriers, enclosures or some type of acoustical material. Barriers are large panels that interrupt the direct “line of sight” from the noise source to the receiver. Technically, the barrier acts as a reflective surface. The noise is reflected off of the surface and back at the source. An example of these are the barriers seen along highways that “separate” the road from residential areas. Barriers are effective when the noise source or the receiver is too big to enclose in a structure. When the noise source is small enough to permit the construction of barriers on all sides of the source, the barrier effectively becomes an enclosure.

Enclosures are used either to contain the noise emitted from a source or to protect a receiver (usually a person) from the noise source. Enclosures are specifically designed structures that reduce the amount of transmitted sound power impinging on the space of interest. In either barriers or enclosures, passive control is achieved by the use of an acoustic absorbing material or sound reflection.

An absorbing material is used in this context to describe the material’s ability to attenuate or “absorb” the sound’s incident pressure wave, thus reducing the amplitudes of the transmitted and reflected pressure waves. The resulting sound pressure level on the opposite side of the absorbing material will therefore be reduced. The absorbing material is something as simple as a metal or plastic panel, or as elaborate as a multilayered partition which consists of specially engineered acoustic foam, different thicknesses of panel layers, as well as different panel materials.

Sound reflection occurs when the acoustic wave is reflected back toward the source by the material. The incident and reflected pressure waves are almost equal, while the transmitted pressure wave is relatively small. This results in a low transmitted acoustic sound power. A material with a significantly greater impedance than the surrounding medium, in which the acoustic wave travels, will cause reflection. Hence no noise will pass through the enclosure. In order for a material to have sound reflecting properties that will provide effective noise attenuation in most settings, the material must be very dense, and very thick. This results in a massive, heavy enclosure. It is the purpose of this investigation to develop an optimal design of a

functional and practical enclosure. Since the enclosure is intended to be small and light, the direct effects of reflection will therefore not be discussed.

The light weight, close fitting enclosure will have some attenuation of the radiated sound due to the mass of the structure. Its effectiveness will also depend on the source to panel distance, the stiffness of the enclosure material, the enclosure panel vibration and the panel thickness. The optimally designed enclosure will have specific material properties and panel thickness depending on the sound pressure level noise spectrum.

This investigation will address the effectiveness of an enclosure used to reduce the acoustic pressure developed by a commercial portable generator. It will focus on the selection of the primary material used in the construction and the geometry of the enclosure. Enclosures are, ideally, sealed environments. Intuitively, any opening or gap in the enclosure allows sound to pass uninterrupted and is detrimental to the function of the enclosure. It is usually physically impossible to have a completely sealed design. Allowances have to be made for cooling, piping and wiring egress. Methods such as silencers and the removal from the “line of sight” between the source and the receiver can be employed to minimize the effects of these required openings of an enclosure.

1.1 Motivation -- The need for a generator enclosure

The motivation of this investigation is to develop an optimal acoustical enclosure for a portable generator using passive noise control techniques. With the population’s ever growing interest in outdoor activities, and our demand for creature comforts during power outages, the use of portable generators is increasing. Even though these items of convenience are beneficial to our enjoyment of life, they are extremely loud. In an effort to develop a commercially appealing enclosure to reducing the radiated noise of the generator, this investigation will define precise design methods intended to optimize the performance of a passive enclosure for a generator. The primary focus will be upon the prediction of the insertion loss of the enclosure, cooling and heat transfer requirements, cost and material selection.

The design of an effective enclosure that can be applied to any size of portable generator is a practical application which also has a commercial demand. It is the intent of this investigation to develop a computer code that will suggest material properties and panel thickness of an enclosure given the required over all dimensions of the enclosure and design constraints such as weight, cost and desired insertion loss. The enclosure is intended to be easily fabricated from commercially available materials. This type of project requires the mixing of several mechanical engineering disciplines. There is the acoustics, the heat transfer, active control, optimization theory and material science.

1.2 Thesis Organization

Chapter 2 will review the bulk of the literature review focusing on the theory of sound waves impinging on boundaries and its components of incident, reflected and transmitted pressure

waves. It begins with the basic theory of an incident pressure wave on a plate and the effects that the plate has on the transmitted wave. Transmission loss theory is discussed which leads to the more practical discussion of insertion loss. The effects of changing material as well as the geometry of the enclosure and how they effect insertion loss is discussed.

Chapter 3 develops the insertion loss model which is used for the optimal design later in the study . The characteristics of the model are explained, such as the effects of varying the material properties and changing the source to panel distance of the noise source.

Chapter 4 describes the optimization code used to design the enclosure. The development of a pattern search optimization technique is presented. A performance index is created and a discussion of the effects of weighting functions and penalty functions is presented. Heat transfer modeling and prediction are also discussed. The model is used to estimate air intake/exhaust opening sizes and estimated air flow necessary for cooling purposes. Chapter 4 also presents the results of the optimization code and the insertion loss prediction. These results indicate the design tradeoffs between material selection and physical enclosure dimensions.

Chapter 5 presents the results of an enclosure prototype fabricated to test the insertion loss model. The enclosure prototype is used to compare actual data against the theoretical data. Chapter 5 also presents results and observations made during this project. Future work is also discussed.

Chapter 2

Literature Review

The primary objective of this review is to acquaint the reader with classical and less well known discussions of passive acoustical control through insertion loss of a panel. This begins with studies in transmission loss and advances to more recent developments in insertion loss. Early model developments in transmission loss are presented, then a discussion of the text book theory of incident, reflected and transmitted pressure waves. A discussion of the differences between transmission loss and insertion loss is also presented. Next, there is a discussion of the principles of insertion loss with enclosures. The theory of insertion loss is viewed from text book application to a more specific study of close fitting enclosures. This includes the effects of the enclosure's vibrations on the performance of the enclosure. To increase the insertion loss of an enclosure, the effects of acoustical material and perforated panels and how they relate to insertion loss is also presented.

2.1 A Review of Sound Transmission Theories

Much of the interest in the study of transmission loss through panels began in the early 1900's. An elementary theory in transmission loss was published by Buckingham, (1924) where

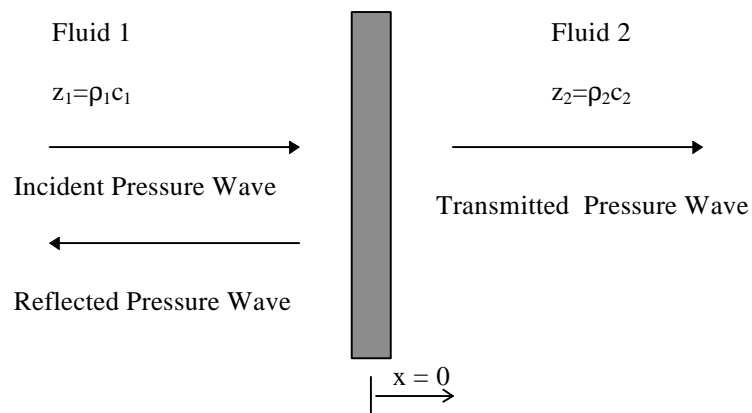


Figure 2.1: Pressure Waves Normally Incident on a Pan

he defined transmission loss as the \log_{10} of the ratio of transmitted to incident pressure waves on a surface. Figure 2.1 is a representation of incident and transmitted pressure on a surface. This representation is only for normal incidence even though a noise source can produce random incidence on a surface. The equation for pressure waves on a surface is complex and varies over frequency and position. It is further complicated by the effects of the multiple degrees of incidence on the surface. Since computations were done by hand, the early models that were developed are quite

simplistic and do not incorporate boundary conditions, nor the effects of random incidence of noise on a surface or its directivity (Crocker, 1994).

Several more studies were conducted over the next twenty five years which further developed the transmission loss theory. These studies included theories of infinite panel dimensions which eliminated the accounting of the boundary constraints. Further investigation during this time lead to the development of theories for the transmission of sound through partitions which incorporated the now well known mass law term, ρ_m , of the panel. This accounting of the mass effect of the panel was developed by Beranek (Beranek et al., 1949). After Beranek's developments in transmission loss theory, London advanced the theory one step further by including the mechanical impedance of the pane (London, 1950). This is one of the first accounts of incorporating the vibration of the panel in predicting the transmission loss. Since then, there has been more development in the details of transmission loss theory which have incorporated the effects of resonant and non-resonant transmission through panels (Crocker, 1994). More recently, the effects of panel modes have also been incorporated into the science of predicting sound transmission (Oldham et al., 1991).

With the invention of computers which are capable of multiple computations, the ability to simulate acoustic behavior through mathematical analysis has become more successful and subsequently more useful. Methods like mode simulation analysis, statistical energy analysis, finite element analysis and boundary element analysis have become some of the more popular techniques used in recent years (Crocker, 1994). Since it is the goal of this investigation is an optimal design of an enclosure, which requires a prediction of the insertion loss, some details of the mathematical models will be reviewed.

2.1.1 Transmission Loss Prediction

The propagation of sound begins with the vibration of a fluid. The vibration of the fluid produces pressure waves. When a propagating pressure wave is interrupted by an infinite barrier, the incident pressure wave is dispersed into two new waves. The infinite barrier is used because it eliminates the need to account for diffraction of the sound around the edges of the barrier. Some of the wave is reflected back toward the source and some of the wave is allowed to pass through the barrier. The part of the wave that is reflected back is referred to as the reflected pressure wave and the part of the wave that is allowed to pass through the barrier is called the transmitted pressure wave. Figure 2.1 shows the representation of this conservation of force per area, or conservation of pressure analysis. These three basic pressure terms are used to discuss the effects of barriers and enclosures.

Transmission loss is generally used to describe the amount of sound reduction, in dB units, that a partition imparts to the transmitted acoustic wave. Many text books such as Fahy (1989), Beranek et al. (1992) and Kinsler et al. (1982) provide apparently simple mathematical models to approximate transmission loss. These models are for the ideal cases of infinite panel dimensions and do not include boundary conditions.

To explain the infinite panel, text book theories on transmission loss, it begins with the mathematical expressions to describe the incident, reflected and transmitted pressures. It is important to discern the incident side and the transmitted side of a barrier. Figure 2.1 illustrates the effects of a barrier on an incident pressure wave at normal incidence. The mathematical expressions are

$$p_i = P_i^{j(\omega t - k_1 x)} \quad \text{at } x = 0 \quad (1a)$$

$$p_r = P_r^{j(\omega t + k_1 x)} \quad \text{at } x = 0 \quad (1b)$$

$$p_t = P_t^{j(\omega t - k_2 x)} \quad \text{at } x = 0 \quad (1c)$$

respectively, where k_x is the acoustic wave number and P_x is the amplitude of the wave. Because the acoustic wave number is defined as $\frac{\omega}{c}$, the incident and the transmitted wave have the same frequency but different acoustic wave numbers if the two mediums have different $\rho_0 c$, or acoustic impedance values. Starting from eq.1, two expressions for the conservation of pressure and the conservation of particle velocity can be developed using conservation of forces. These are respectively:

$$p_i + p_r = p_t \quad (2a)$$

$$u_i + u_r = u_t \quad (2b)$$

where u is the normal velocity of the pressure wave and is defined as $\frac{\pm p}{z}$, depending on the direction of propagation of the wave, and where z is the impedance of the fluid. Therefore the continuity of normal velocity equation can be rewritten as

$$\frac{p_i - p_r}{r_1 c_1} = \frac{p_t}{r_2 c_2} \quad (3)$$

The transmission loss coefficient is defined as the ratio of the incident pressure to the transmitted pressure. This ratio, defined as the transmission loss coefficient t , is

$$t = \frac{|P_i|^2}{|P_t|^2} \quad (4)$$

The transmission loss of the panel is then

$$TL = 20 * \text{Log}_{10} \left(\frac{1}{t} \right) \quad (5)$$

This is the expression that defines transmission loss in terms of the impedance of the fluid mediums. Using Newton's law, $\Sigma F = \Sigma m * a$, the pressures on the panel, the mass, and the acceleration of the panel, the transmission loss can be expressed in terms of the panel's surface density and frequency. In complex notation the acceleration of the panel is

$$\dot{v} = j\omega \frac{P_x}{\rho c} \quad (6)$$

Then applying Newton's law

$$(p_i + p_r - p_t)S = r_{panel} h S \dot{v} \quad (7)$$

where S is the surface area of the panel and h is the thickness of the panel. Assuming that the two fluids are the same, and using the continuity of normal velocity equation the pressure wave amplitudes become:

$$P_r = P_i - P_t \quad (8)$$

Using equations. 7 and 8 and resolving for the ratio of the incident pressure to the transmitted pressure the reciprocal of the transmission loss coefficient becomes

$$\frac{P_i}{P_t} = \left(\frac{m * j\omega}{2 * z} \right) + 1 \quad (9)$$

where m is the surface density of the panel. Squaring the magnitude of each side to eliminate the complex part of the equation, this ratio becomes

$$\left(\frac{1}{t} \right)^2 = \left(\frac{m\omega}{2z} \right)^2 + 1 \quad (10)$$

The transmission loss in terms of the mass of the panel and the frequency is

$$TL = 10 * \text{Log}_{10} \left(\left(\frac{m\omega}{2z} \right)^2 \right) \quad (11)$$

The addition of unity in equation 11 is relatively small to $\left(\frac{m\omega}{2z} \right)^2$ term, and can be ignored in the log term of the transmission loss equation. In order to determine the transmission loss using this mass controlled method the surface density, m, and the bulk modulus or effective stiffness of the material, B, of the panel are necessary.

$$m = \rho_{\text{panel}} * h \quad (12)$$

$$B = \frac{E_{\text{panel}} * t^3}{12(1 - \nu_{\text{panel}}^2)} \quad (13)$$

Next, the critical frequency of the panel is calculated

$$f_c = \frac{2}{c} \sqrt{\frac{B}{m}} \quad (14)$$

The transmission loss using the “single-panel” method (Beranek et al, 1992) is predicted using the following equations.

$$TL = 20 * \text{Log}_{10} \left[\left(\frac{2\pi \left(\frac{f_c}{2} \right) f_c m}{2\rho c} \right)^2 \right] - 5 \quad (15)$$

$$TL = 10 * \text{Log}_{10} \left[\left(\frac{2\rho f_c m}{2rc} \right)^2 \right] + 10 * \text{Log}_{10} \left(\frac{2h}{p} \right) \quad (16)$$

According to the theory in Beranek, the slope of the transmission loss for frequencies below $f_c/2$ is 6 dB per octave and is predicted using eq.15, while the slope of the line for frequencies above f_c is 9 dB per octave and is predicted using eq.16. Figure 2 is a plot of the predicted transmission loss of a single panel vs. frequency. The area of the curve below the half critical frequency is called the mass controlled region. This is because the amount transmission loss that the panel will provide below this frequency is controlled by the mass of the material. The area of the curve between the half critical frequency and the critical frequency is called the critical frequency. The transmission loss is decreased in this region due to a panel resonance. The area above the critical frequency is called the damping controlled region. This is because the amount of transmission loss that the panel will provide is primarily dependent on the internal damping of the panel material.

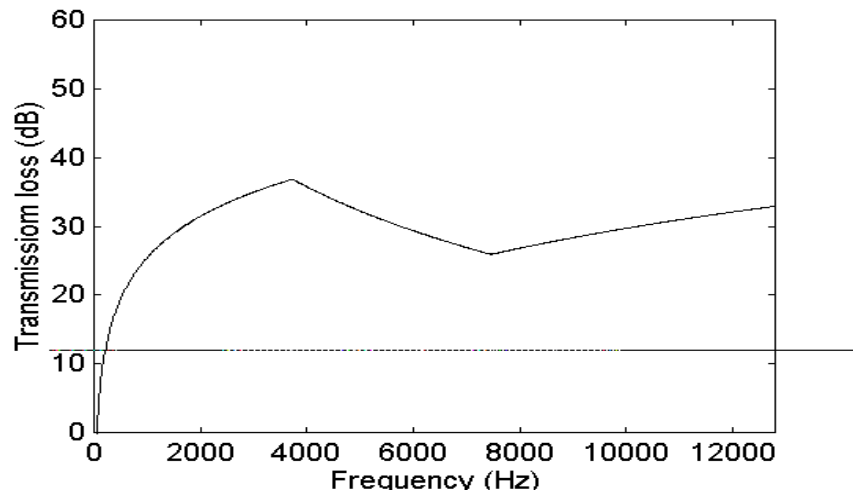


Figure 2.2: Predicted Transmission Loss of a Single Partition

To increase transmission loss, a doubled walled system can be implemented. This type of configuration has two panels separated by a gap. The gap is usually filled with a sound absorbing material to further enhance the transmission loss. The equations to predict transmission loss of a double panel system are developed in the same manner as the single panel, except now x is constrained to the fixed distance, d , separating the two walls. Kinsler and Fray (Kinsler et al., 1982) show a thoroughly detailed development of these equations. To simplify these equations, text book theory states that the transmission loss of a double panel system where the acoustic impedance surrounding both panels is the same, is simply the transmission of one panel plus the transmission loss of the second panel, which is:

$$TL = 10 * \text{Log}_{10} \left(\left(\frac{m_1 \mathbf{w}}{2z_1} \right)^2 \right) + 10 * \text{Log}_{10} \left(\left(\frac{m_2 \mathbf{w}}{2z_2} \right)^2 \right) \quad (17)$$

However, a double partition does not always increase the sound transmission loss at every frequency. The double partition may be less effective than each of the single partitions individually at low frequencies. At low frequencies the double partition acts as if were a single-degree-of-freedom resonator system (R.Y. Vinokur, 1996). London predicted the resonant frequency of the two panel system with the equation:

$$f = \frac{1}{2p} \sqrt{\frac{rc^2 M_1 M_2}{(M_1 + M_2)g}} \quad (18)$$

where g is the thickness of the air gap and M_1 and M_2 are the surface densities of the layers (London, 1950). The double layer partition becomes an effective mass-spring-mass system and the result is extremely detrimental at low frequencies (Vinokur, 1996). This effect was especially prevalent for small gap distances between panels, such as those found in close fitting enclosures.

The text books theories also assert that the transmission loss can be determined by adding the transmission losses of each of the single panels together with the transmission loss of the

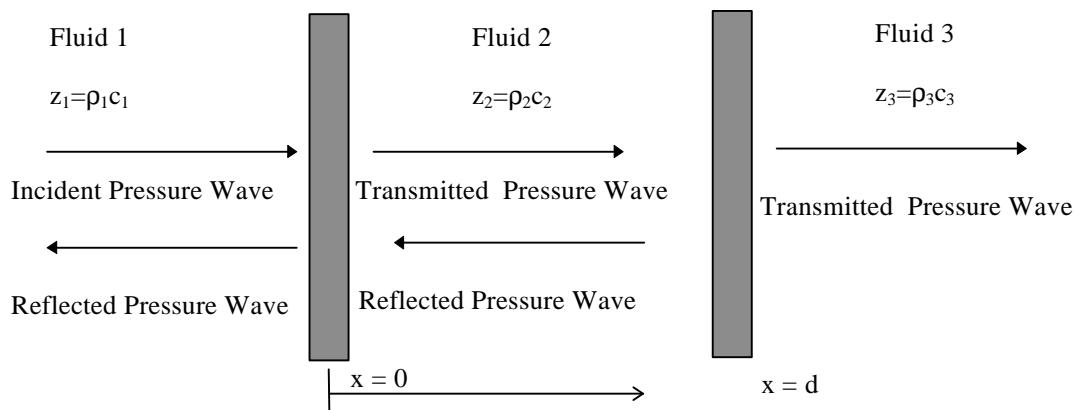


Figure 2.3: Pressure Waves Normally Incident on a Double Pane

material in the gap between the panels (Beranek, 1992, Kinsler et al., 1982, Fahy, 1985). These discussions of double walled enclosures also assume no mechanical coupling between the two panels. This is an ideal case and cannot be fully realized in the fabrication of an enclosure. This results in Figure 2.4 show the predicted transmission loss of a double panel enclosure made from aluminum with air as the fluid between the panels.

The transmission loss of double partitions varies from 6 dB greater for a tightly coupled walls to 20 dB greater for loosely coupled partitions as compared to single walled partitions (Rettinger, 1973). Closely coupled partitions are double walls that are separated by a few inches, while loosely coupled partitions are separated by several feet.

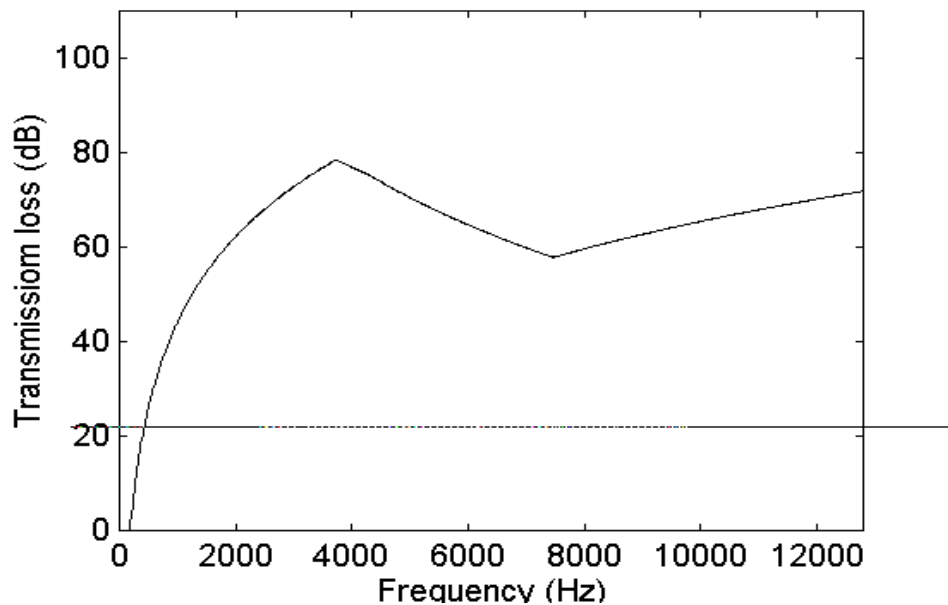


Figure 2.4: Predicted Transmission Loss of a Double Panel

With ideal conditions of completely “de-coupled” walls, the transmission loss adds as Beranek suggests only for frequencies over 1000 Hz (Rettinger, 1973).

Once the predicted values of transmission loss have been calculated, is a simple task of subtracting the transmission loss dB from the noise source dB to calculate the source sound pressure level when the double panel is implemented. If this calculation was applied to an enclosure using suggested levels of transmission loss predicted in fig. 2.4, it would be indicative of an enclosure that could virtually silence any noise source. However, the theory of transmission loss that is discussed in most books has been developed for large, semi-infinite panels that separate large room volumes and have ideal boundary conditions.

Transmission loss is somewhat impractical when discussing the effects of an enclosure because it focuses on the pressure wave immediately before and immediately after the panel surface which is also assumed to be completely rigid. The near field effect of the noise source on the enclosure panel forces the panel to vibrate. The panel surface behaves as a non rigid wall

which is subject to many modes of vibration. It is difficult to measure the incident and transmitted pressure waves without the use of sensitive measuring equipment. It is more beneficial and practical to view the enclosure or barrier from the perspective of insertion loss.

2.2 A Review of Insertion Loss

Insertion loss is the reduction, in dB, of the sound pressure level or sound power level of a noise source. It is more effective, and measurable, than the transmission loss of an enclosure. To measure insertion loss, an array of microphone positions are used around a piece of machinery or equipment. Sound pressure level measurements are taken with the equipment operating. The enclosure is then applied and the same sound pressure level measurements are taken again. There is no need to get measurements of incident and transmitted pressures. As long as the measurements are taken in the same locations and the background noise is taken into account, insertion loss measurements are rather simple.

The use of an enclosure is frequently limited by the space surrounding the equipment. The enclosure is considered “close fitting” when the noise source to panel dimension is usually less than 1 meter. It has been found that predicting insertion loss using the typical text book, or architectural methods as they are sometimes referred to, is impossible. The acoustical field inside the close fitting enclosure does not behave the way it would in a large room. There is considerable coupling between the noise source and the enclosure (Oldham et al., 1991). Relatively few sources have presented equations that deal specifically with close fitting enclosures. This is due to the difficulty in accurately modeling enclosure dynamics and the coupling between the noise source and the enclosure.

Several empirical studies have been performed to predict the effects of an enclosure. Jackson has several articles dealing with the performance of acoustic hoods (Jackson, 1962 and Jackson, 1966). His studies were conducted using two panels. One was used as a vibrating noise source while the second plate represented the enclosure. Jackson’s model derived an expression for the insertion loss as a function of the vibration level of the noise source panel. As Oldham criticized in his paper, the insertion loss, however, is not a function based solely on the vibration of the panel (Oldham, 1991).

As with transmission loss, many text books present theoretical models to predict insertion loss in an architectural sense. That is to say that the theories are based upon room acoustics and large “enclosed” areas. The models are infinite and theoretical and the effects of source to panel distances as well as boundary conditions are still ignored. Fahy and Beranek, both discuss insertion loss with a one dimensional infinite area model (Fahy, 1985, Beranek, 1992).

2.2.1 A Text Book, Close Fitting Insertion Loss Model

Insertion loss is similar to transmission loss with respect to material thickness, density and stiffness. The denser and thicker the panels of the enclosure are, the more transmission loss there will be in the mass controlled region. For low frequencies, greater stiffness leads to more insertion loss there will be in the stiffness controlled region. As discussed earlier, the models used

in room acoustics will not be accurate in predicting the performance of an enclosure due to the fact that the noise source occupies most of the enclosure volume (Bryne, et al., 1988). This leads to one of the two most important topics when predicting insertion loss of a close fitting enclosure. It is the effects caused by the excited modes of the enclosure. The other important topic is related to the frequency dependent interference between the incident and reflected waves at the boundary.

Several papers address the elastic panel response when predicting insertion loss. Junger found it difficult to accurately predict the excited modal response of an enclosure (Junger, 1970). Tweed and Tree also had models for predicting the performance of close fitting enclosures, but were also unsuccessful (see review in Bryne, 1988). Jackson's model, which is only a function of the vibration of the panel, showed a reduction in the predicted noise spectrum. However, the model suffered from large negative insertion loss values at the enclosure panel modes (Jackson, 1966). His work showed a reduction in the insertion loss at frequencies where half of the wavelength occupied the enclosure (Oldham, 1991). Crocker also addresses this difficulty in predicting insertion loss. Crocker describes that at low frequencies the modes of the panel effectively cancel each other out except at the corners of the enclosure and are called corner modes. As the frequency increases the modes still cancel out except along the edges and these he calls edge modes. As frequency still increases above the critical frequency of the panel the surface modes are not canceled on the panel and the surface becomes an effective radiator of sound at these modes. The enclosure becomes useless at these frequencies because the enclosure panel transmits the noise and in some cases increases the sound pressure level at these frequencies causing a negative insertion loss (Crocker, 1994). Roberts (1990) proposed that the critical frequency of the panel can be determined using the following relationship:

$$f_c = \frac{Kc^2}{h} \sqrt{\frac{\rho_m}{E}} \quad (19)$$

where the constant $K = .555$, h is the panel thickness, c is the speed of sound in air, ρ_m is the material density and E is the Young's Modulus (all variables are in metric units) .

One of the more recent models for the prediction of insertion loss of a close fitting enclosure is presented by Oldham (1991). He too includes the effects of panel modes into his model. He presents two types of models, one for a simply supported boundary condition and one for a clamped boundary condition. He states that there is never a truly clamped condition nor a truly simply supported boundary conditions and therefore a true boundary condition lies some where between the two models.

Oldham's initial assumption in his modeling efforts is that the enclosure is subjected to a uniform field inside the enclosure. This means that the noise source is driving the panel behaves like a single degree of freedom piston and the pressure will be uniform across the panel (Oldham, 1991).

Oldham studied the composition of the panel modes that affected the insertion loss of the enclosure. He assumed that the only mode that would radiate noise is the 1:1 mode shape. The higher order modes exhibits what he called a "sloshing" effect. This means that the higher order modes effectively canceled each other out and did not radiate noise. The effects of the 1:1 mode on the insertion loss is a pronounced dip at the frequency which equals the panels fundamental

resonance frequency. There are more dips in the insertion loss above the fundamental resonance frequency, but these are caused by cavity resonance frequencies. Cavity resonances occur where the particle velocity inside the enclosure is exciting the panel in such a manner where as the panel velocity is in phase with the noise particle velocity and has approximately the same amplitudes. This condition forces the enclosure panel to become an effective radiator of the noise source, and there is almost no attenuation of the noise sound pressure level, causing a drastic null in the predicted insertion loss at these frequencies. More specific details of this will be discussed and shown in Chapter 3.

Oldham's model will be shown to be quite useful in predicting the insertion loss of an enclosure, but it is still not quite accurate. Engineers and designers of acoustical enclosures still rely heavily on the use of actual test data due to the fact that the enclosure and the source are strongly coupled by the fluid of the medium, the cavity has complex pressure waves that are difficult to model and the dimensions of the enclosure are small enough that the cavity sound fields do not agree with statistical models (Fahy, 1985). It is also more beneficial to investigate the overall sound pressure or power level as a performance index of an enclosure (Oldham, 1991). It will be shown later that this performance index makes Oldham's model more useful in its prediction of sound pressure level than any others examined in this study.

2.3 Acoustic Absorbing Materials and Perforated Panels

Although it is not the focus of this investigation of acoustic enclosures and insertion loss, it is necessary to discuss the importance of absorbing acoustical material because it can help attenuate the lower frequencies that a single paneled enclosure cannot. This material is usually a porous material, like foam, which is used to insulate a surface from transmitting sound waves. The performance of the acoustic material is determined by knowing the absorption coefficient of the material.

The absorption of the material depends mainly on the impedance of the material. There is also some dependency on how the noise strikes the material's surface. Some materials are not as effective when trying to attenuate noise that strikes the surface at oblique incidence angles. The absorption coefficient is frequency dependent. A material can have a high absorption in a given frequency band width, thus producing a great deal of insertion loss. Outside of this band width, the absorption coefficient might be negligible (Walker, 1971). By adding absorbing material the enclosure could be tuned to attenuate a more specific frequency range.

Determining the absorption coefficient of acoustic material is probably more difficult than determining the insertion loss of a panel. The performance of an acoustic material liner is based on the impedance of the material. It is difficult to predict this with out actually testing the material. From research observations, semi-empirical formulae have been developed (Bolton et al., 1993). These models have limited success in predicting the actual insertion loss that the material will provide.

The vibration of the structure also effects the absorption of the material. The amount of attenuation that foam will provide is related to how the foam is attached to the enclosure panel.

Bolton discusses his observations of introducing an air gap between the acoustic foam and the panel. The performance of the foam is five times better when the foam is separated from the panel by a 1 mm air gap compared to the foam being directly attached to the panel itself (Bolton et al., 1993).

The use of perforated panels backed by an air space to attenuate low frequency noise has also been investigated. The perforated panel and the air space become a resonator type muffler system. The perforated panels have small diameter holes that are spaced far apart relative to the hole diameters. Maa develops mathematical models to predict the performance of perforated and double perforated panels (Maa, 1987). His model determines the acoustic impedance of the panel based on material properties and perforation density.

Jinko and Swenson show experimental results using a perforated wall for sound reduction of noise in a room (Jinko et al., 1992). Their model is based on the model developed by Maa. They found that this type of noise attenuator is more resilient to a harsh environment than acoustic foam. They also showed that the perforated panel has an absorption coefficient close to 1 for low frequencies with normal incidence. Their work showed that even in room acoustics, the panel vibration effects the performance of the acoustic absorber.

The use of acoustic foam or perforated panels would enhance the acoustic attenuation capabilities of the enclosure. However it is the purpose of this investigation to determine the interaction between the noise source and the enclosure to predict the insertion loss and design an optimal enclosure using a simple panel. Once an optimal design is predicted, techniques developed to determine the optimal acoustical lining could be used to improve the performance of the enclosure. To achieve this, more extensive modeling and testing will have to be performed to develop a model for predicting the insertion loss of a complex panel consisting of a base material, acoustic liners and perforations.

Chapter 3

Developing the Insertion Loss Model

In this chapter, the development of a specific insertion loss model is used to determine the radiated sound pressure level outside a close fitting enclosure. The model is developed for an enclosure that is constructed of a solid, single panel layer. The effects of material properties, panel dimensions and the noise source to panel distance are investigated. Theoretical and measured data from a test apparatus are presented and differences between the two are discussed.

3.1 A Practical Insertion Loss Model

Insertion loss is a more practical method to analyze the effects of an enclosure on a noise source since it is a direct comparison of the sound pressure level from the noise source with and without the enclosure. Insertion loss is defined as the base ten logarithm of the square of the ratio of the acoustic sound pressure level without the enclosure to the acoustic sound pressure level with the enclosure. Methods to predict insertion loss usually include the prediction of transmission loss in the development of the equations (Beranek et al., 1992). This explains why there is mass law and stiffness effects in current mathematical models of insertion loss. The prediction method for this work closely follows the theories and models developed by Oldham (1991) His work is heavily concerned with the vibration of the enclosure panel caused by the acoustic pressure from the noise source. This model is influenced not only by the material properties of the panels, but also by the distance the panels are from the noise source.

To date, researchers have found that it is impossible to predict the effects of a close fitting enclosure using previously developed room acoustic techniques (Oldham et al., 1991). Most theories do not consider structural affects or source-to-panel distance considerations and how these variables effect the insertion loss. Oldham has a detailed study into the prediction of a close fitting enclosure where the source-to-panel spacing is less then 1 meter. Since the noise source and the enclosure panels are so close, they are considered to be in the near field. For a sound to be in the near field the acoustic wave number times the distance from the noise source to the panel is much less than unity (i.e. $k d \ll 1$)

Oldham develops two different type of theoretical models, one for a simply supported panel and the other for clamped boundary conditions. Since no enclosure will exhibit ideal simply supported or clamped boundary conditions, Oldham suggests that the solution corresponding to the actual boundary condition lies somewhere between the two. There is only a slight difference between the two models and it is difficult to distinguish between the two except at frequencies below 2.5 kHz. It will be seen later that for this test case, the clamped boundary condition model was fairly close to actual data taken for the model used in this experiment.

Oldham suggests that the effects of structural excitation are an important consideration in developing a model. Certain structural modes of the enclosure are excited from the noise and cause the panels to vibrate. The vibration of the enclosure panels effectively becomes a vibrating piston. This response of the structure can increase or decrease the insertion loss depending on the frequency of the excited mode and the frequency content of the noise in the enclosure. If the

panel vibrates in phase with the incident pressure wave, the transmitted pressure is virtually unaffected by the enclosure. A cavity resonance might produce a pressure that is greater than the driving pressure which results in a negative insertion loss. These excited resonate modes will cause the structure to vibrate and produce a new pressure wave, adding to the pressure wave emitted from the noise source. This results in a increase in the transmitted pressure and a negative insertion loss.

As the panels are excited by higher frequencies from the noise source, higher modes of the panel are excited. The higher order mode shapes will, however, essentially cancel their effects , causing them to be ineffective at radiating sound. (Oldham at al., 1991) Therefore, Oldham’s model assumes that the 1:1 mode of the structure is the only effective radiator of sound.

His model also assumes that a close fitting enclosure will experience a uniform pressure field over a large frequency range. (Oldham at al., 1991) In his discussion, the source is assumed to be a vibrating panel which is positioned close to the enclosure panel. The enclosure panel is therefore exposed to uniform pressure over the. The sound transmitted through the enclosure is effected by three variables:

- the impedance of the excited cavity
- the mechanical impedance of the panel
- the coupling between the two

(Oldham at al., 1991). This means that the noise source creates pressure waves in the medium inside the enclosure and the medium, in this case air, excites the panel to vibrate. If the particle velocity of the enclosure panel vibration is approximately equal to the particle velocity of noise source, the panel will be ineffective in preventing sound transmission. If the panel particle velocity is relatively slow or out of phase with the noise source particle velocity, the panel will be very effective in preventing sound transmission. So how the panel vibrates in response to the excitation by the noise source, strongly influences the performance of the enclosure.

The insertion loss of frequencies below 2kHz is controlled by the effective stiffness (or bulk modulus) of the material while the insertion loss of the high frequency is controlled by the material properties, density and internal damping, as well as the distance of the noise source to the panel. The effects of these variables and how they are coupled together will be discussed later in section 3.3.

Oldham developed two models for two different types of boundary conditions, simply supported and clamped. The simply supported model is

$$IL = 10 * \log_{10} \left[\left(\cos(kd) + \left(\frac{\pi^2}{4K\omega\rho_0c} \right) * \sin(kd) \right)^2 \right] \quad (20)$$

where:

k is the acoustic wave number, d is the distance from the source to the panel

ρ_0c is the impedance of the fluid around the panel (in this case it is the impedance of air)

and

$$K = \frac{\left(\frac{16}{\rho^2}\right)}{\left[D_i \rho^4 \left(\frac{1}{a^4} + \frac{1}{a^2 b^2} + \frac{1}{b^4}\right) - \omega^2 r h\right]} \quad (21)$$

where D_i is the complex bulk modulus,

$$D_i = \left(\frac{E h^3}{12(1-\nu^2)}\right)^* (1 + i\eta) \quad (22)$$

and a is the length of the panel, b is the width of the panel, ρ is the density of the panel, η is the internal damping coefficient of the material, h is the thickness of the panel and, E is the Modulus of Elasticity or Young's Modulus of the material.

For the derivation of the clamped boundary condition model, the equation approximately the same as the simply supported case. The difference is in the K term of his equation, which is developed from the modes of the panel. A simply supported panel will have different modes than a clamped panel. For a detailed explanation refer to his paper (Oldham et al., 1991). For the clamped boundary condition case the model to predict insertion loss is the same as Equation 20 and:

$$K = \frac{(1.35)}{\left[3.86 * D_i \left(\frac{129.6}{a^4} + \frac{78.4}{a^2 b^2} + \frac{129.6}{b^4}\right) - \omega^2 r h\right]} \quad (23)$$

Figure 3.1 is a plot of the two models developed by Oldham. The only real difference is the first null in the insertion loss.

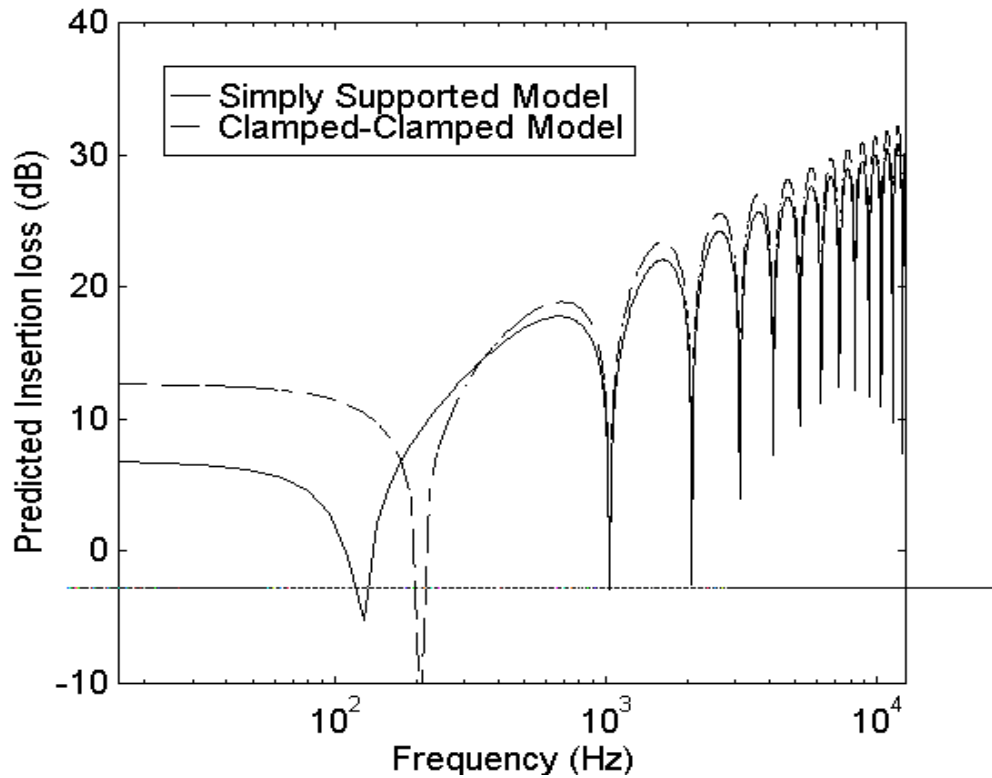


Figure 3.1: Predicted Insertion Loss for Clamped and Simply Supported Models

This difference in the two models is caused by the different first fundamental modes for a clamped and simply supported panel. The nulls after the first one are caused by the source-to-panel distance. What causes the depth of these nulls in the insertion loss needs to be discussed in detail. It is the values of these nulls which will control the overall insertion loss of the enclosure.

3.1.1 Test Apparatus to Compare the Model to Test Data

A test apparatus was constructed to compare actual insertion loss to the predicted model presented by Oldham. The apparatus consisted of two aluminum boxes. One of the boxes was a cube with dimensions 26.7 x 26.7 x 26.7 centimeters and will be referred to as the inner box. The other box was 29.2 x 29.2 x 29.2 centimeters and will be referred to as the outer box. Both boxes were only five sided so that they would fit together with the outer box covering the inner box with a 1.2 centimeter gap between the two boxes on all five sides. A six inch mid range speaker was used as the model noise source which was used to produce white noise from 0 to 12.8 kHz. The speaker and the boxes were placed on the floor of an anechoic chamber for testing purposes. The speaker was placed facing up so that the noise was directed straight upward. Figure 3.2 shows the orientation of the speaker and the test box.

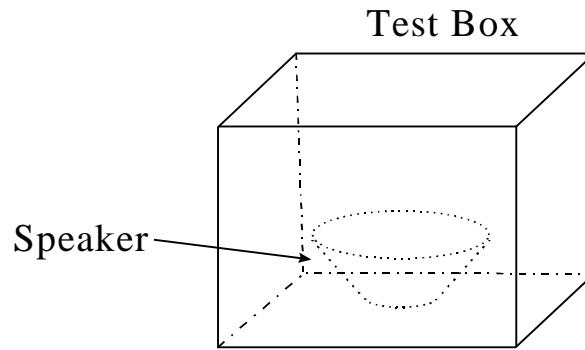


Figure 3.2: Test box speaker orientation

Tests were performed using a B & K microphone and a Hewlett Packard signal analyzer to record data. Several sound pressure level measurements were taken without the enclosure, with the outer and inner box individually, and with both boxes together. Several microphone positions approximately 1 meter away from the enclosure were used to record sound pressure level measurements around the noise source.

3.1.2 Measured Insertion Loss Values

The model was compared to actual test data using the test boxes described above. Figure 3.3 is the comparison of the clamped insertion loss model proposed by Oldham to actual data using a single box. It was found that by using a double box configuration

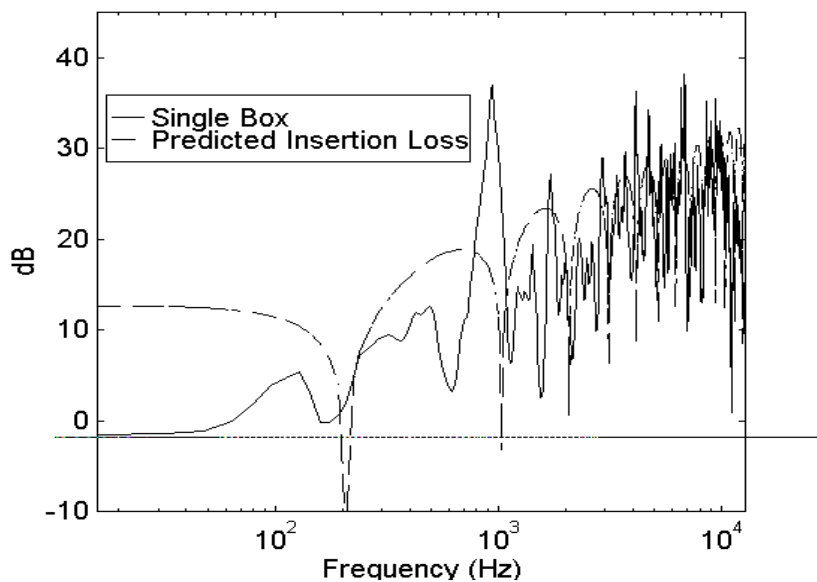


Figure 3.3: Predicted vs. Actual Insertion Loss for Clamped Boundary Conditions

there was only an effectively doubling of the mass which resulted only in a 6 dB increase in the insertion loss.

The general trend as well as the predicted sound pressure levels in dB of the predicted and the actual insertion loss are similar. However, there are some differences between the nulls in the predicted model and the actual data that will be discussed.

As discussed earlier, the model developed by Oldham, which is used here, is influenced by the fundamental mode of the panel only. He concluded that higher order modes did not effect the insertion loss as much as the 1:1 mode. The effects of the first mode modified by the stiffness of the backing cavity according to Oldham, correspond to the first null in the predicted and actual insertion loss. There is a slight difference between the two nulls, but that is because the test case is not truly a clamped boundary condition. And as Oldham stated, the actual model will be in-between the clamped and simply supported models presented. At about 1000 Hz there is a peak in the actual data, but the model predicts a null in the insertion loss. Testing different source to panel distances by moving the speaker up and down inside the box, effected the frequency and amplitude of this peak, proving that some higher order modes are effecting the insertion loss. Never the less, for a general application this model is correct in its trends of actual insertion loss, and will be assumed to be a fair predictor of insertion loss.

3.2 Constraints on The Model

The first null in the predicted insertion loss is caused by the effective 1:1 mode of the panel. In section 3.3, the frequency of the first null will be shown to be determined by the enclosure panel dimensions. The higher frequency nulls are controlled by the distance that the panel is from the noise source. These effects will also be discussed in Section 3.3. The constraints placed on this model deals with the depths of the nulls in the predicted insertion loss.

Oldham has discussed what causes the nulls but neglected to distinguish how low the nulls should be. Mathematically the nulls are calculated when the term contained in the bracket of Equation 20 is less than one. For these values, the insertion loss will be negative. Therefore the nulls are calculated when:

$$\left(\cos(kd) + \frac{\pi^2}{4K\omega\rho_0c} \sin(kd) \right)^2 < 1 \quad (24)$$

To find the extreme minimums of the nulls, it is necessary to determine when Equation 24 = 0.

$$\left(\cos(kd) + \frac{\pi^2}{4K\omega\rho_0c} \sin(kd) \right)^2 = 0 \quad (25)$$

Simplifying Equation 25, the extreme minimums of the nulls are determined when:

$$\tan(kd) = \frac{-4K\omega\rho_0c}{\pi^2} \quad (26)$$

A plot of Equation 26 against Equation 20 using the clamped boundary conditions of Equation 22 and 23 is shown in Figure 3.4. The solid line is the insertion loss model and the dashed line

represents Equation 26. From the figure it can be seen that the nulls occur when Equation 26 is approximately equal to zero. If the resolution of the figure was increased, it can be seen that at the frequencies where Equation 26 equals zero, the insertion loss would be negative infinity. When applied to a generated noise sound pressure level, it would predict that with the enclosure the radiated sound pressure level would be positive infinity. This is obviously incorrect and intuitively impossible!

Depending on the material property values and the resolution of the frequencies, the values of the nulls will fluctuate greatly. Referring To Figure 3.3, it appears that the minimum values of the nulls increase as frequency increases. But a closer look at the higher frequencies reveals that this is not true. A slight change in a panel value or change in panel dimension will change the value of the nulls.

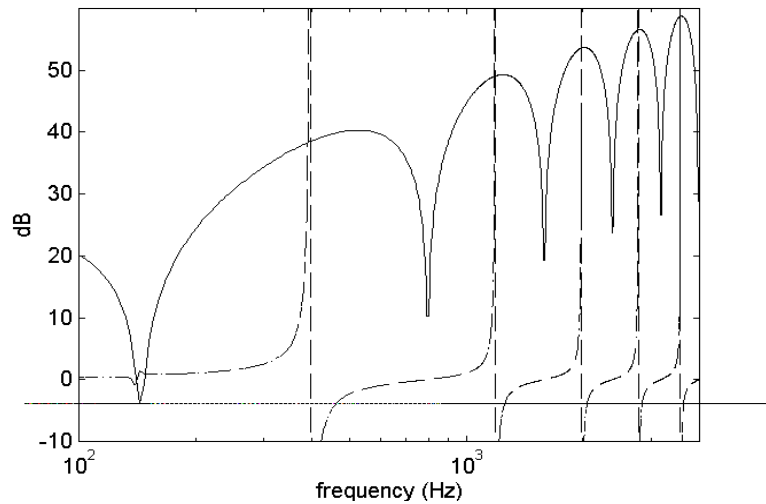


Figure 3.4: Plot of Insertion Loss Null Prediction vs. Insertion Loss Model

Predicting the nulls in the insertion loss is extremely important in determining the predicted sound pressure level. The predicted sound pressure level outside the enclosure is the radiated sound pressure level from the noise source minus the insertion loss. The nulls in the insertion loss model become peaks in the predicted sound pressure level. Figure 3.5 shows the effects of the insertion loss model on a simulated sound pressure level.

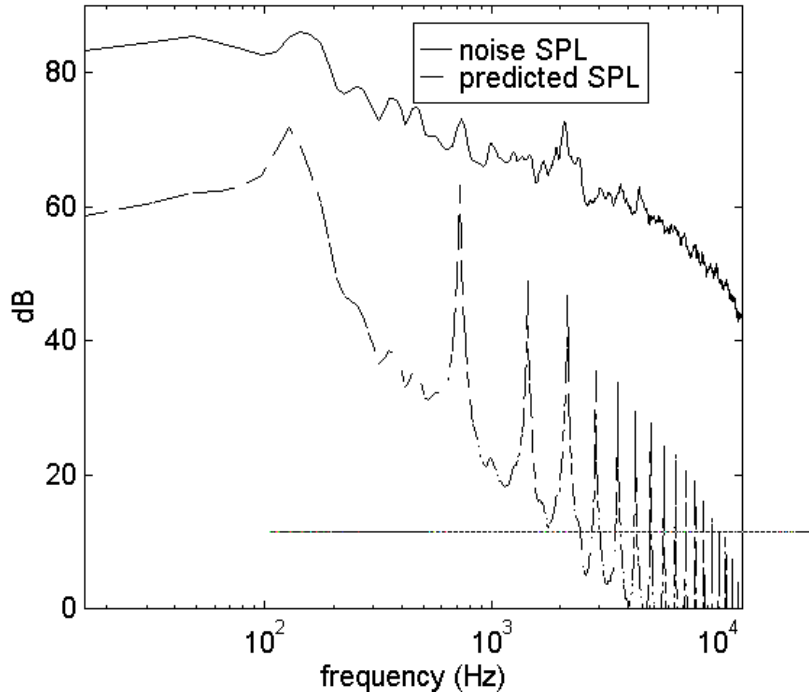


Figure 3.5: Predicted SPL, Calculated from the Insertion Loss Model using a noise SPL spectrum

The peaks in the predicted insertion loss are the values that control the over all sound pressure level because they dominate the overall sound pressure level calculations. The overall sound pressure level is calculated using the following expression:

$$SPL_{total} = 10 * \log_{10} \left(\sum_{1}^n 10^{\left(\frac{SPL_n}{10} \right)} \right) \quad (27)$$

where SPL_n is the sound pressure at the nth frequency. Since the over all sound pressure level is part of the performance index used in the optimization code discussed in Chapter 4, it is necessary to constrain the peaks produced by the insertion loss model. This will be beneficial in predicting an overall sound pressure level that changes because of material and enclosure properties, not because of mathematical resolution in the model

As the pressure wave from the noise source excites the panel at cavity and panel resonances, the panel vibrates in phase with the acoustic particle velocity. This is what allows the sound to be transmitted almost unaffected by the enclosure. As discussed earlier, at the fundamental panel resonance, the acoustic particle velocity is actually increased by the panel

vibration. As the frequency increases, so does the acoustic particle velocity and the enclosure experiences higher cavity resonances. The result is the dip in the insertion loss. The enclosure panel velocity cannot vibrate as fast as it is being forced to by the incident pressure waves as the frequency increases. There is still a dip in the insertion loss at these frequencies but the particle velocity of the panel cannot equal the acoustic particle velocity, and as frequency increases, the effect of the panel vibration becomes less severe.

The minimum value of the insertion loss dips are not controlled by the mathematical model. They are a result of a logarithm of a value less than one. In order to control these dips, a constraint routine was used in the enclosure insertion loss computer coding. The dips were limited to a 20 dB drop from the preceding maximum. This limitation is based on two factors. First, this reduction will make the second null in the insertion loss approximately zero for all material. This means that the second null of the insertion loss will provide no attenuation of the transmitted noise. This is a reasonable assumption since the panel velocity is capable of still being equal to the acoustic particle velocity at this low frequency. Secondly, the work performed in the thesis by James Mumaw from Virginia Tech, showed that the acoustic response of the enclosure was 20 dB down from the disturbance noise.(Mumaw 1996)

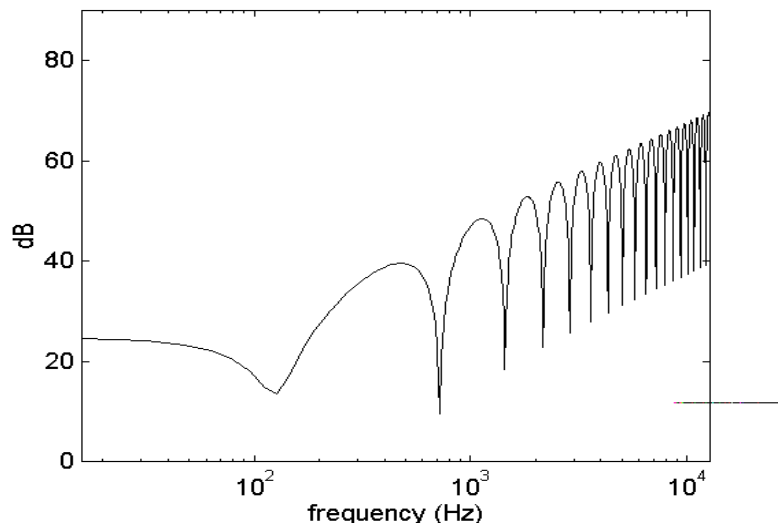


Figure 3.6: Constrained Insertion Loss Model

Constraining the insertion loss nulls will ensure an over all predicted sound pressure level that varies only on material properties and dimensions. Figure 3.6 shows the result of this constraint placed on the insertion loss model. By constrain the minimum value of each null, the prediction of the insertion loss has a distinct and repetitive upward trend. This makes this model effective in the optimization code because the overall SPL will increase or decrease with the

movement of the insertion loss curve. The overall SPL will not vary depending on the frequency resolution used to sample the data or the material property values .

3.3 Effects of Material Properties and Panel Dimensions on the Model

The next several figures show the effects of varying panel properties on the insertion loss prediction. In each case there is an increase in one of the variables. This is depicted in each figure with the solid line being the smallest value, the dashed line the middle value and the dash-dot line being the largest value used in each representation.

Figure 3.7 shows the effects of increasing the panel size on the insertion loss. Only the first null is effected by the change. As the panel gets larger the frequency of the first mode will decrease, hence the decreasing first null frequency. The nulls at the higher frequencies, which did not change, are influenced by the source-to-panel distance.

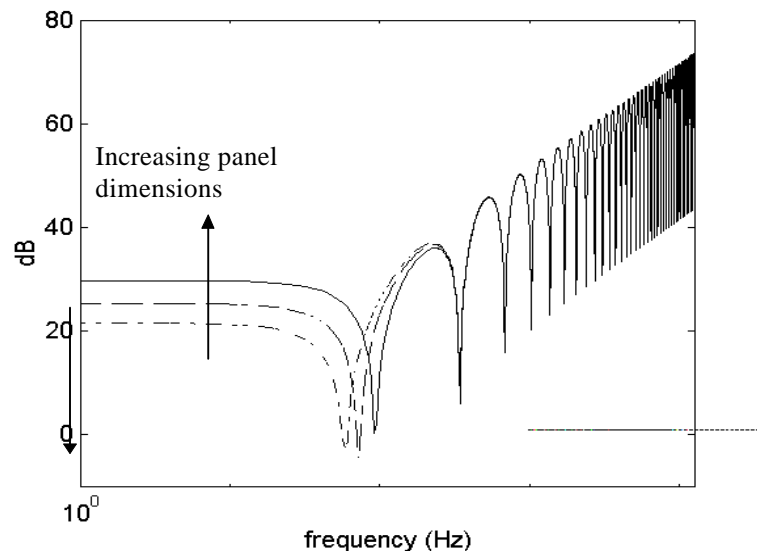


Figure 3.7: Effects on Insertion Loss Due to Changes in Panel Dimensions

The insertion loss model development is also heavily influenced by the source-to-panel distance. Depending on the distance from the source to the panel will determine the frequencies of the cavity resonances and resulting nulls in the insertion loss. Figure 3.8 is a plot showing the effects of increasing the source-to-panel distance. Note the movement of the nulls of higher frequencies as the source-to-panel increases. The first null caused by the first mode of the panel is relatively unaffected by the change in the source-to-panel distance. There is less insertion loss at this first null as the distance increases, but the frequency at which the null occurs does not change.

A further investigation of the insertion loss model was necessary to understand the effects of changing material properties and how these changes would effect the insertion loss. By using the program to predict insertion loss and varying panel thickness and panel density.

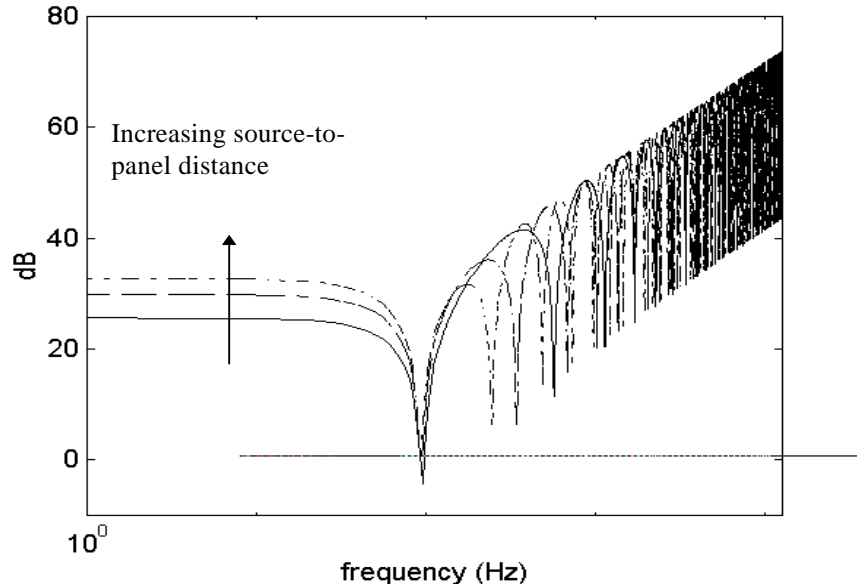


Figure 3.8: Effects on Insertion Loss Due to Changes in Source-to-Panel Distance

By increasing the panel thickness the amount of insertion loss is increased at the lower frequencies as shown in Figure 3.9. This is due to the fact that the insertion loss at low frequencies is controlled by the effective stiffness of the panel. The effective stiffness is a function of the Young's modulus, poisson's ratio and the material thickness as described by Equation 13. By increasing the panel thickness the effective stiffness is increased and the result in an increase in the insertion loss. The first null, which is controlled by the 1:1 mode, is also increased by increasing the effective stiffness. These responses are expected according to text book theories of insertion loss and panel mode shapes.

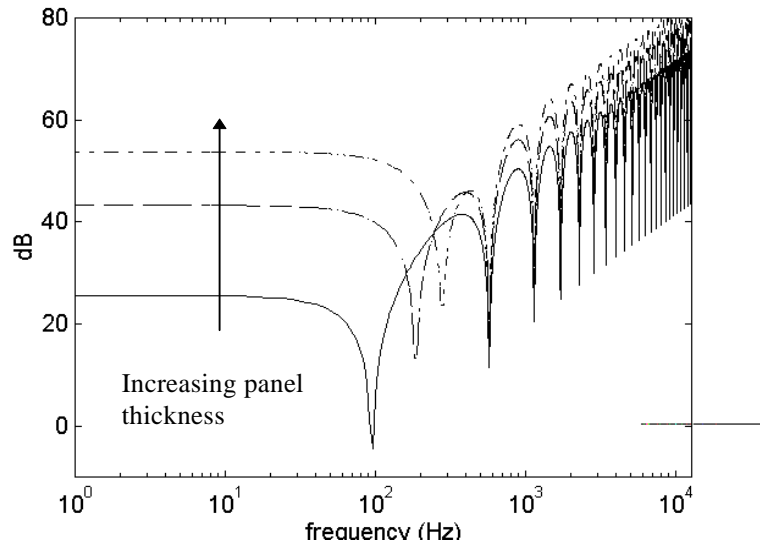


Figure 3.9: Effects on Insertion Loss Due to Changes in Panel Thickness

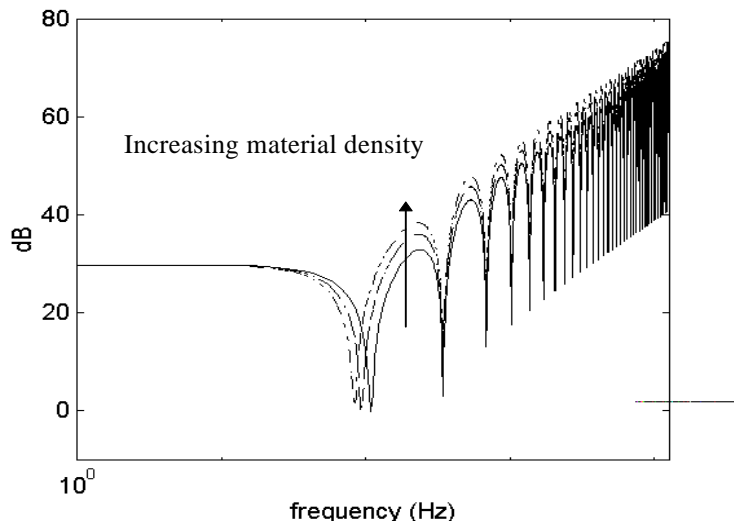


Figure 3.10: Effects on Insertion Loss Due to Changes in Panel Density

Figure 3.10 shows the effects of increasing the panel density. With a denser panel the frequency of the 1:1 mode is decreased. The resulting insertion loss in the higher frequencies is also increased. This too follows text book theories that state the insertion loss will increase at higher frequencies with density.

3.4 Test Comparison of a Prototype Enclosure with the Generator to the Insertion Loss Model

With a thorough understanding of the mathematical model, a comparison of the predicted insertion loss, radiated sound pressure level and over all sound pressure level was conducted. A prototype enclosure for the generator was constructed using plywood. The dimensions of the wood enclosure are 66 x 43 x 46 cm. Since the generator is an engine, considerations to let the engine breathe were made. A hole measuring 7.5 x 20 cm was cut on one side of the enclosure to allow for the exhaust to be vented out. On the opposite, a 15 x 25 cm hole was cut to allow for cooling air to enter the enclosure. It is already assumed that the performance of the wood as an acoustic hood will be poor, but it will be beneficial it applying the model to an actual test case.

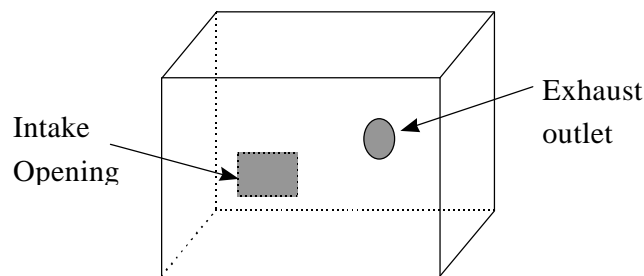


Figure 3.11: :Intake and exhaust openings on the test enclosure

These holes are obviously going to be places where the sound is allowed to pass without interference which is degrading to the insertion loss. The actual and predicted insertion loss and resulting sound pressure level measurements will not be exactly equal because the model assumes an ideal enclosure that is tightly sealed. However the general trend between the actual and predicted insertion loss should be similar.

The sound pressure levels were measured in dB(A) scale in an IC engine laboratory using the Hewlett Packard Signal analyzer and the B & K microphone. Measurements were taken on all sides of the generator at a distance of one meter. The measurements were then averaged to achieve an over all sound pressure measurement. This test was conducted with and with out the enclosure while the generator was under no load. Figure 3.12 shows the A weighted sound pressure measurement of the generator in the lab without the enclosure. This results is a 108.5 dB(A) overall sound pressure level measurement.

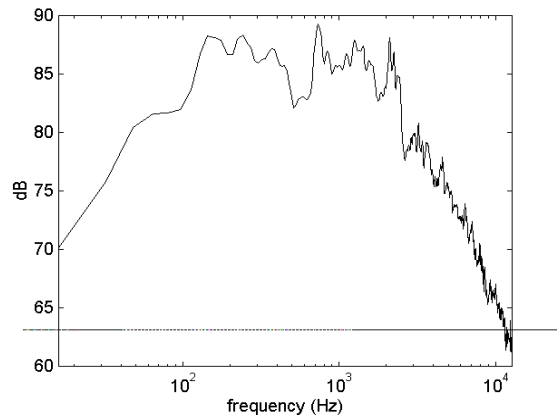


Figure 3.12: Measured, Sound Pressure Level of the Generator in the Lab

The enclosure was then placed over the generator and the same measurements were taken. Figure 3.13 is a comparison of the A weighted sound pressure levels of the generator with and without the enclosure.

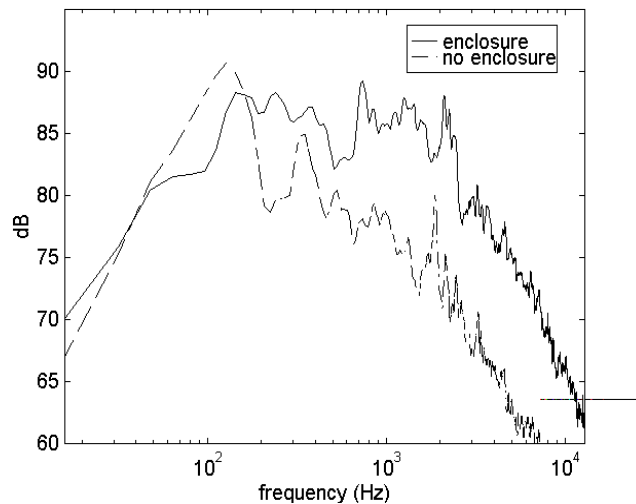


Figure 3.13: SPL of the Generator With and Without the Enclosure

There was an actual increase in the radiated sound pressure level around 100 Hz. This was caused by the effective 1:1 mode of the enclosure. The resulting over all sound pressure level with the enclosure was 101 dBA, which was a 7 dBA reduction.

The actual and predicted insertion loss is shown in Figure 3.14. Note the pronounced dip in the measured and predicted insertion loss caused by the fundamental mode. Unfortunately, the

holes had a severe impact on the insertion loss. Above 1000 Hz the insertion loss was approximately 10 dB. More efforts will have to be made to eliminate direct holes into the enclosure. Although this will not be a solution to the problem, it will help to improve the insertion loss.

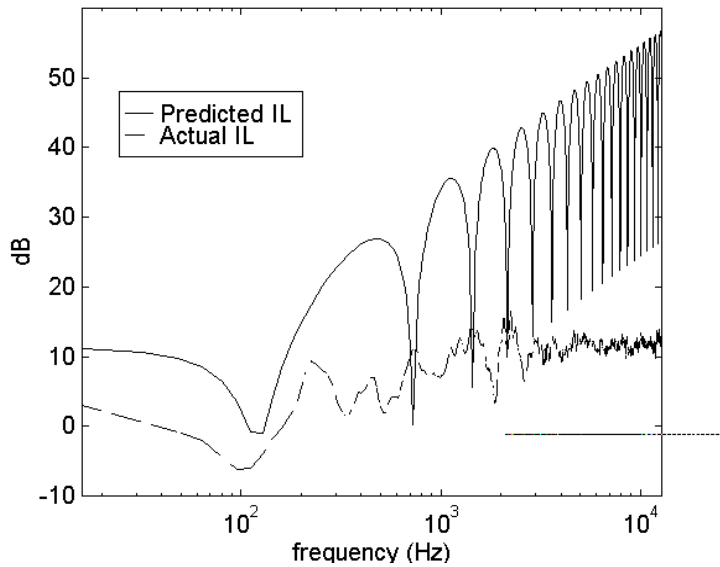


Figure 3.14: Actual and Predicted Insertion Loss for the Prototype Enclosure

Although the insertion loss model fared poor when predicting the insertion loss of the enclosure for the generator, it was an adequate method when the enclosure was sealed. This was seen with the use of the aluminum test boxes. The model still predicts the general trend of the insertion loss provided by the enclosure and will be used in the optimization design code.

Chapter 4

Design Methodology

Chapter 4 is a discussion of the optimal engineering design technique used in presented. Chapter 4 also discusses a heat transfer model required for the design of the enclosure and the considerations necessary for intake and exhaust air flow.

There are several text book methods for determining the optimum of a mathematical model. The optimum is either the minimum or maximum of the function depending on what is desired. Most text books describe virtually the same methods with only slightly different names. James Siddal (1982) outlines several of the classical methods to optimal design engineering. These methods range from linear programming to more advanced methods of calculus. However, despite all of the advanced mathematical methods, the simplistic methods are sometimes still the best method to use. The simple methods make programming the optimization logic in computer code much easier. These models also take less computer time because the computations are less involved. One of the most simple yet effective methods, especially with the help of a computer, is a search method.

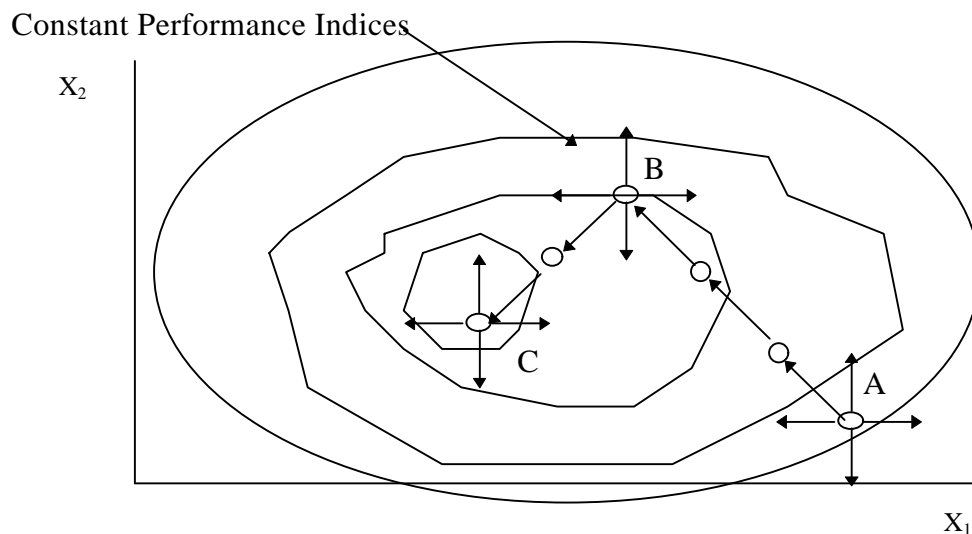


Figure 4.1: Example of a Pattern Search Method

The optimization technique used in this experiment was the Hook and Jeeves method or pattern search. It is one of the most successful types of numerical optimization and probably one of the easiest since it avoids complicated and numerous derivatives (Siddal, 1982). With the

advantage of computers, it is also one of the quickest methods, and is only slowed by the processing speed of the computer.

This search method uses a type of contour map and “lay of the land” type search pattern. Figure 4.1 will be helpful in briefly explaining the pattern search method. As with any optimal design search, a performance index is determined. This performance index can be a function of several design variables and the sum of several equations. For this experiment, the performance index is composed of the overall sound pressure level and the weight of the enclosure, and will be discussed later. For the example in Figure 4.1 there are only two design variables, X_1 and X_2 . To start the search, an initial value is assumed. This is point A in Figure 4.1. From this initial value “steps” are taken in all directions. From point A, the performance index increases for the X_2 variable with a positive step, represented by an upward movement. The performance index also increases with a negative step represented by a leftward movement for the X_1 variable. This movement upward and to the left is now referred to as the pattern of the optimization search. The program will keep taking the pattern step until the performance index stops increasing. In Figure 4.1, the performance index stops increasing at point B. At this point the program will determine a new pattern to follow. Hence the change in direction to point C in Figure 4.1. And again at point C the program will calculate the performance index again by taking a step in all directions and a new pattern step will be determined.

At point C in Figure 4.1 arise one of the main difficulties in this type of search technique. If the step size is too large, the maximum value will be “missed” by the search code. If the contour of the surface was more complex and there was a local maximum, the search program would get stuck here using the current step size thinking it found the optimized value of the performance index. Careful consideration must be given to the process of determining the step size of each design variable and adequate measures must be used to avoid local minimums and maximums. Also, some consideration must be given in determining the step sizes to avoid “missing” the maximum value. With these basics of the pattern search method, the optimization code can be discussed.

4.1 Development of Pattern Search Optimization Code

This optimization technique was chosen for several reasons. First and foremost is the complex nature of the equations that predicts insertion loss. Due to the fact that there are several variables which can be considered design variables, the pattern search method can be modified to search on any or all of the design variables. The variables that can be considered design variables are the panel thickness, the material density, the Young’s modulus of the material, Poisson’s ratio and the internal damping coefficient of the material. The enclosure dimensions could also be considered design variables, but they were considered fixed to the outer dimensions of the generator in this experiment. The second reason is that the overall sound pressure level, which is the value that is of most importance, is dependent on the noise spectrum of the noise source. A “good” enclosure design will avoid having the nulls of the insertion loss at the same frequencies as peaks in the noise sound pressure spectrum. It is the intent of this optimization process to be able to apply the program to a variety of noise spectrums. The program therefore loads a noise

spectrum, calculates an insertion loss over the same frequencies as the given noise spectrum and then the overall predicted radiated sound pressure level is calculated.

The optimization program begins with a graphical user interface (GUI) developed using MATLAB. This is shown in Figure 4.2. It allows the user to customize the optimization search. The GUI is composed of several editable text boxes that let the user define the initial starting points of the design variables. It also allows the user to set the minimums and maximums that the design variables are allowed to reach. The GUI

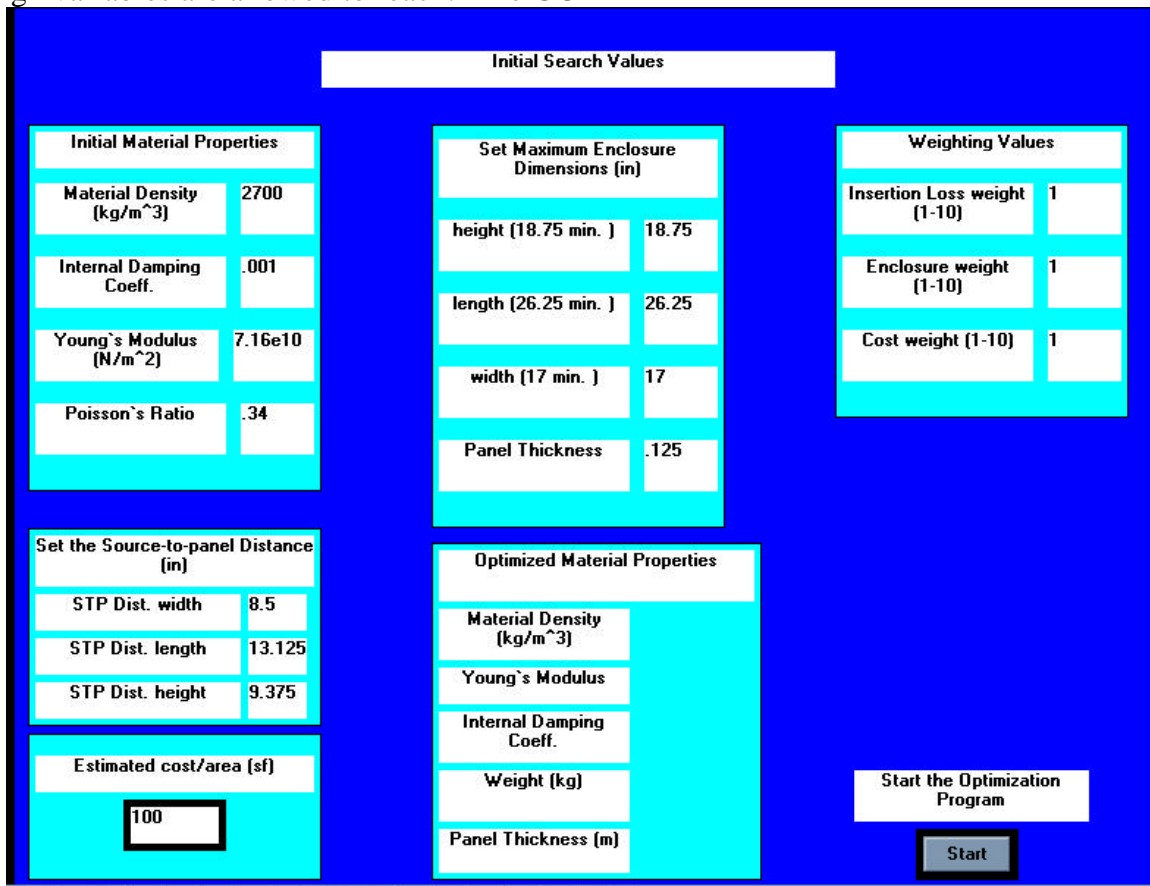


Figure 4.2: Optimization GUI

allows for the maximum dimensions of the enclosure to be set. In future work using this code, these variables can be used as design variables instead of constants. Because the program is set up as several *.m files that are initially called in the run_file.m file, the process to modify the code is rather simple. The enclosure dimensions were set in this investigation because it was determined that the enclosure would not be larger than the generator frame itself. The GUI has a set of parameters that allow the user to set weighting values on the performance index. Once the code determines the optimum enclosure properties, it displays the solution in the GUI.

The step sizes of the optimization code were very important. The pattern search method lends itself to get caught in local minimums or maximums. In order to avoid this, the code performs several calculations when determining the optimum step size. The optimization code

has a set step size value set for each design variable. This is set internal to the code. The step file then calculates the performance index using a positive step and a negative step. To avoid being caught in a local minimum, the code calculates the performance index again using a step size larger than the set step size. The set step size is multiplied by the square root of the iteration that the code is currently calculating. So for the third iteration, the step file could calculate the performance index using a positive and negative set step size as well as a positive and negative step equal to the set step size times $\sqrt{3}$ (for the third iteration). To safeguard against the optimization process from missing the optimum by “over stepping” the optimum value, the code also calculates the performance index using a value that is less than the set step size. In a similar manner, the code determines a step size that is smaller than the set step size. How much smaller depends on the iteration that the code is calculating. This is done in order to close in on the optimum. As the process progresses, and the code is zooming in on an optimum, the step sizes get smaller and smaller. The code has flags set that determine how small to let the step sizes become. If the step sizes become too small, the step value is set to zero and if all the step sizes of the design variables reach zero, the process will end finding the optimum value.

4.1.1 Performance Index: Considerations and Sensitivity

The first concern in beginning the optimization process is determining the performance index. This is the value that will be optimized. For this experiment, there are several possibilities of performance indices. The intuitive index is the overall sound pressure level. Choosing this standard for the performance index would lead to the obvious solution. The enclosure would become as thick and as dense as set in the computer program because a massive enclosure would eliminate almost all radiated noise.

The performance index has to be based not only on the overall radiated sound pressure level, but the total weight of the enclosure. There will be some point at which the predicted sound pressure level will not change as much with the increasing weight of the enclosure. Since it is the goal of this enclosure design to minimize the radiated noise as well keep the weight of the enclosure to a minimum, the optimization will search for the minimum performance index. That is to say that it will search for a performance index that is composed of the minimum radiated sound pressure level and the minimum weight of the enclosure. The optimization code is set up to consider the cost of the enclosure as a part of the performance index but it is not used here.

By placing more emphasis on the overall sound pressure level will yield a thicker, denser and thus heavier enclosure. The more emphasis stressed on the overall radiated sound pressure level will yield heavier and more massive enclosures that have very low radiated sound pressure levels. Placing the emphasis on the overall weight of the enclosure will yield a light enclosure that has poor acoustic capabilities. The sensitivity of the performance index is controlled by variables called weighting parameters.

4.1.2 Weighting of Parameters -- Cost, Insertion Loss, Weight

Weighting parameters control the direction of the optimization search. In this optimization process, the GUI offers a panel to set the weighting parameters for cost, insertion loss and weight. The weighting parameters chosen for the example of the optimal enclosure design were unity. This means that weight and the overall radiated SPL were treated equally. In this investigation the performance index is:

$$PI = SPL_{oa} * SPL_{weight} + Enclosure\ Weight * Weight_{weight} \quad (28)$$

where SPL_{weight} and $Weight_{weight}$ are the weighting parameters and SPL_{oa} is the overall sound pressure level.. The weighting values used were both unity. At some point in the optimization search, will not improve as much as the weight increases. This can be shown in the following two figures.

Figure 4.3 shows the calculated performance index for iterations of the optimization code. Here the performance index is a combination of the enclosure weight and the

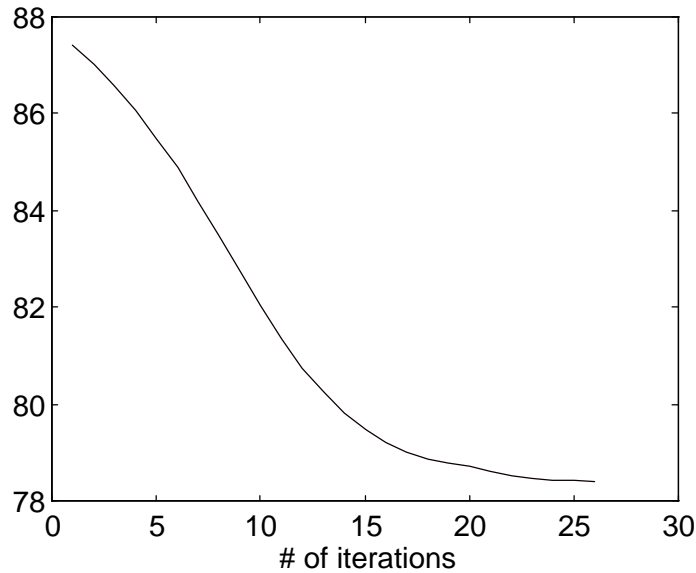


Figure 4.3: Calculated Performance Index for Iterations of the Optimization Code

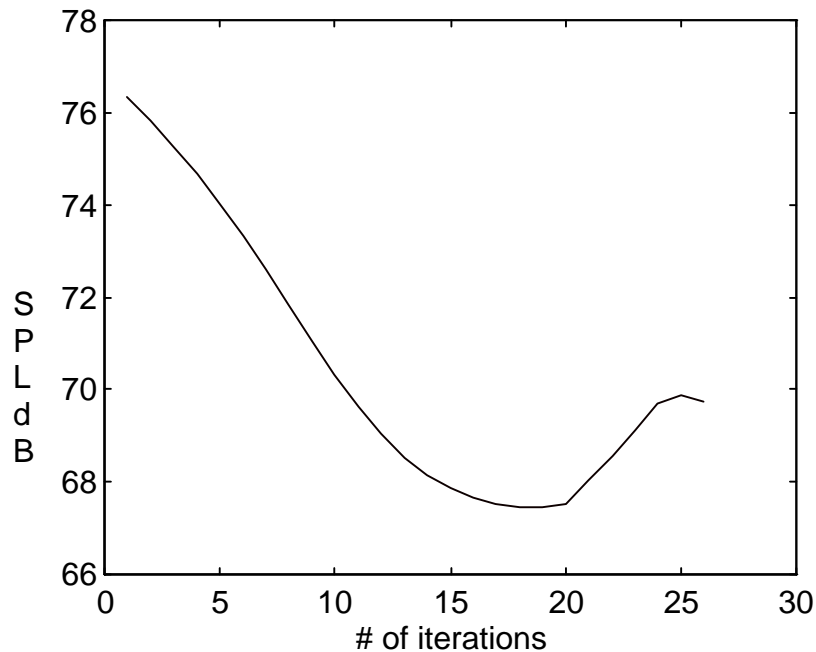


Figure 4.4: Calculated Overall SPL for Iterations of the Optimization Code

radiated SPL. Figure 4.4 is the calculated overall SPL of the enclosure for the same optimization trial.

Notice in Figure 4.4 that the radiated SPL reaches a local minimum approximately at 20 iterations. However, since the weight of the enclosure is part of the optimization process, the performance index in Figure 4.3 is minimized in approximately 26 iterations even though the overall sound pressure level increases after 20 iterations. If the weighting parameter of the weight of the enclosure was reduced to zero, to optimization process would search for the enclosure material properties that yielded the lowest radiated SPL. This would intuitively be the thickest and densest material allowed by the optimization code. If the weighting parameter of the weight of the enclosure were set higher than the overall SPL then the optimization process would find a lighter enclosure with poorer radiated SPL.

4.1.3 Results of the Optimization Code

After several iteration trial processes, the optimization code was perfected. Figure 4.3 already has shown the performance index reaching a minimum value with the chosen weighting parameters set at unity. Depending on the starting design variable values and the weighting parameters, the processes takes approximately twenty five to thirty iterations.

Appendix I shows the un-enclosed sound pressure level of the test generator to be 91.24 dB. Using the optimization code, it is predicted that the radiated sound pressure level can be

reduced to 75.08 dB. A plot of the predicted SPL vs. the measured noise SPL is presented in Figure 4.5. There is a net reduction of 16.16 dB in the SPL. To achieve this reduction the enclosure would have to be made from a material having a density of 1430 kg/m^3 , a Young's modulus of $8.64 \times 10^{10} \text{ N/m}^2$ and a panel thickness of 4.75 mm. The result of the optimization process depends on the noise spectrum supplied to the program and the weights placed on the performance index.

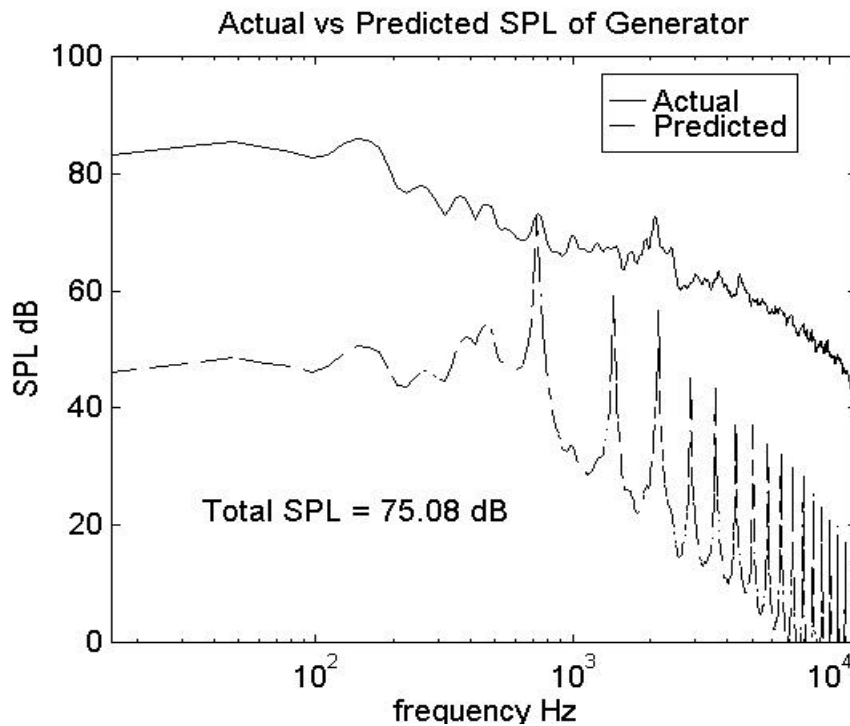


Figure 4.5: Actual SPL vs. Predicted SPL Calculated Using the Optimization Code

With the values that the optimization code yielded, the material for the optimal enclosure in this application would have a Young's modulus that is close to brass and a density that is slightly less than magnesium. Since no single material has the exact material properties, the optimal enclosure design suggests that a composite material would be the best material to use. A composite could be developed to contain the predicted material properties.

4.2 Heat Transfer Model

Up to this point in this project nothing has been discussed about the heat transfer requirements and exhaust and inlet considerations. Therefore, along with an accurate insertion loss model, this design problem requires a heat transfer model. Since the main purpose of this investigation is primarily the insertion loss of a close fitting enclosure, the heat transfer model will

be a typical text book approach with standard assumptions of efficiencies of internal combustion engines and AC generators.

In order to clarify the terms used hence forth, refer to Figure 4.6 showing the parts of the generator.

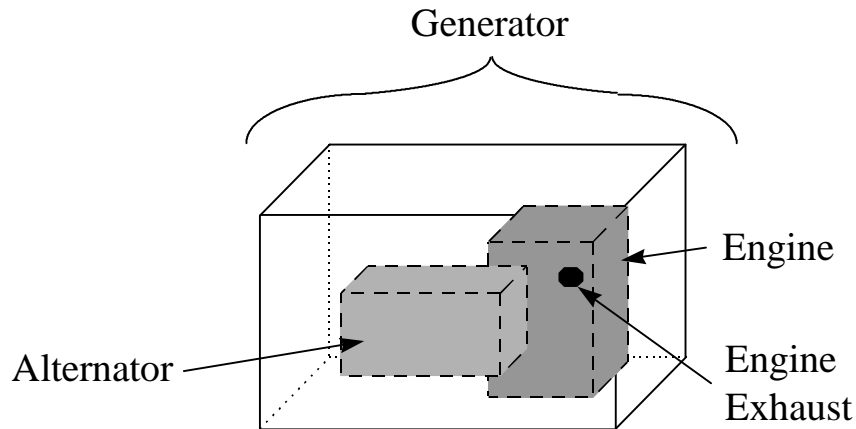


Figure 4.6:Generator Components and Component Location

Initial heat transfer design considerations began with the operating temperatures of the engine, exhaust and generator in a free field environment. A resistance thermocouple was used to measure the operating cylinder head temperature, and a type K thermocouple was used to measure the engine cylinder head operating temperature. Figure 4.7 shows the free field operating temperatures of the cylinder head temperature.

Testing of the generator in the enclosure with no forced air flow and under an electrical load showed that the cylinder head would not reach the maximum operating temperature determined by the engine manufacture, Briggs & Stratton, of 450 degrees F. After operating the generator for 10 minutes under load in the enclosure the cylinder head temperature settled at 370 degrees F.

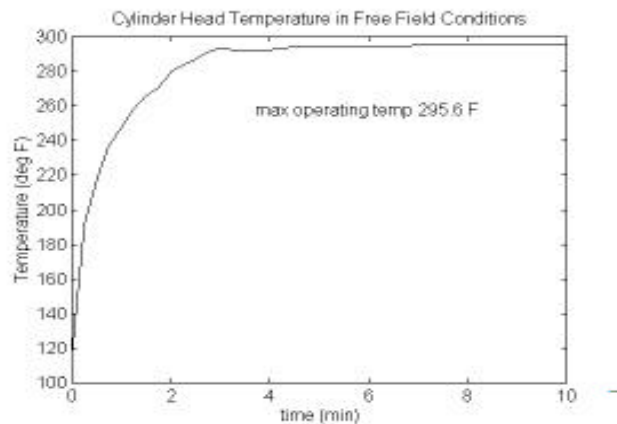


Figure 4.7: Operating Cylinder Temperature Free Field Environment

The operating temperature of the alternator was also measured while the generator was under load inside the enclosure and in free field environments. In free field conditions with an electrical demand placed on the generator, the alternator reached a steady operating temperature of 34 degree C or 93 degree F. While operating under the same electrical load under the wood test enclosure, the alternator operated at 36 degree C or 97 degree F.

As discussed earlier with the wood test enclosure, there were two holes placed in the walls for exhaust and intake considerations. The intake opening would accommodate the intake and the exhaust of the cooling air as shown in Figure 4.8 as the cooling air in and the cooling air out. The alternator and engine both have cooling fans that help draw air into the enclosure and cool the equipment. To determine the required mass flow rate of the required cooling air, a simple heat transfer analysis was performed.

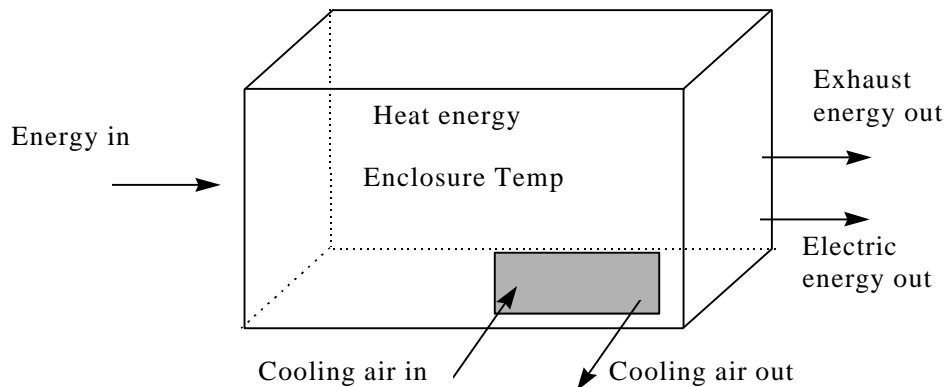


Figure 4.8: Enclosure Energy Balance Diagram

Briggs & Stratton supplied data which said that the engine used .46 gallons per hour when the generator was under $\frac{3}{4}$ load. The generator is rated at 2500 watts and $\frac{3}{4}$ output means that the generator is producing 1875 watts of energy out. The lower heating value of gasoline is 32 kW hr/gallon. If the generator is consuming .46 gallons of fuel per hour, the amount of energy put into the system is 14.7 kilowatts. Assuming that the alternator is 90% efficient the output of the engine shaft into the generator is 2080 watts. Approximating the energy usage of the engine, it is reasonable to assume that the energy that is not used in the work output is divided equally between the heat lost through the exhaust and the heat lost over the surface of the engine. This means that the surface heat energy of the engine is 6.31 kilowatts. Assuming the efficiency of the alternator, the energy lost to heat is 2317-2080 or 205 watts. The estimated amount of heat inside the enclosure is then 6.5 kilowatts of heat energy.

Approaching the problem with a standard heat transfer analysis means that $Q = \dot{m} * C_p * \Delta T$, where Q is the amount of heat energy, \dot{m} is the required air flow and C_p is the specific heat of air at constant volume which is 1 kJ/(kg °C). Assuming a hot day, the outside ambient air temperature would be 98° F or 37° C. Also assuming the air temperature inside the enclosure should not exceed 150°F or 65°C, the required air flow necessary would be 226.5

grams/sec. This would have to be supplied by an inlet fan that could deliver approximately 3 m/s of cooling air flow through an opening that is 10 cm by 10 cm square so as to keep the inlet opening as small as possible. This mass flow rate and velocity seem reasonable since there was no forced cooling air when the wood enclosure was tested and the cylinder head temperature and the alternator operating temperature reached an acceptable steady operating temperature.

4.3 Intake and Exhaust Considerations

With a heat transfer model, intake designs should be discussed. This investigation proposes the use of ducts to direct the flow of cooling air into the enclosure. This would be accomplished with the use of a fan inside the duct. By using a duct, the line of sight through the hole would be eliminated. It would not prevent the transmission of noise through the opening, but it would help to reduce it.

The exhaust was piped out of the enclosure through an exhaust tube. It was one of the reasons for such a poor response with the wood test enclosure. The measurements taken with the enclosure still had the exhaust noise unshielded in the measurement of the overall SPL. For later investigations, the exhaust should be silenced using an expansion chamber muffler that is attached to the outside of the enclosure. Placing the muffler on the outside of the enclosure will not add to the heat energy inside the enclosure.

Chapter 5

Results and Conclusions

The first and foremost part of this investigation that should be addressed is the insertion loss model. The architectural acoustic model that is proposed in most acoustic text books work well in predicting the insertion loss of noise in rooms. Figure 2.2 indicates that with the use of a single partition there is approximately a 35 dB reduction in the transmitted sound pressure level. Standard text book theory states that the use of a double panel partition has twice the effective insertion loss reduction. Figure 2.4 indicates that as much as 70 dB of insertion loss can be achieved by a double panel partition. However, this kind of result is extremely difficult to achieve with a close fitting enclosure.

A practical, effective model that predicts the insertion loss of a close fitting enclosure was paramount to this investigation. Trying to predict the effectiveness of an enclosure using traditional text book applications proved to be unattainable. The clamped boundary condition model developed by Oldham (1991) was accepted for use in this investigation.

Oldham suggested that the fundamental mode of a panel was the only mode that would effectively radiate noise. Figure 3.3 shows how Oldham's model is a fair predictor of insertion loss for a sealed enclosure. There is a pronounced dip in the actual insertion loss at the fundamental frequency but there are also dips at higher frequencies. These higher nulls are a result of the higher modes of the panel, much like Oldham predicted. These higher order, excited modes seem to have a direct relationship to the noise source to panel distance. By testing the sealed, aluminum enclosure with different noise source to panel distances, these nulls from the higher order modes decreased as the speaker was placed closer to the panel.

Oldham's mathematical model is a fair predictor of insertion loss, but it suffers when predicting the insertion loss at the nulls determined by the source to panel distance. Depending on the frequency and the material properties as well as the panel dimensions, the model predicts a negative infinity insertion loss. This results in a positive infinity predicted radiated sound pressure level. This problem was corrected in the optimization code. The fundamental mode is a significant radiator of noise, so it has a slightly negative insertion loss for most panels. As frequency increases, nulls in the predicted insertion loss occur periodically. These nulls are caused when the panel velocity is out of phase with the particle velocity of the noise source. The null was limited to 20 dB down from the preceding peak by the optimization code. Limiting the nulls predicted a more realistic insertion loss. This is shown in Figure 3.6. The 20 dB was chosen for two reasons. First it limits the second null to approximately 0 dB insertion loss. This means that the panel can vibrate with the same velocity as the noise source. The second reason was that James Mumaw (1996) showed that the acoustical response of a duct was approximately 20 dB less than the exciting noise source.

Once a reliable insertion loss model was realized, the optimization code was developed. The design of an enclosure that is acoustically robust but also has a weight factor will ultimately have an optimal design. With the use of weighting parameters, the direction of the optimization code can be controlled. If an enclosure that reduces the overall sound pressure level is desired regardless of the weight, the optimization process will predict a material that is dense, with a high

Young's modulus with the enclosure panel being thick. The optimization process converges on an optimal design in approximately 25 to 35 iterations depending on the initial search values and the weighting parameters. Results of the optimization process for this investigation are shown in Figure 4.3.

A prototype enclosure was constructed out of plywood to compare the insertion loss model with actual data taken with a generator. The general trend of the actual and the predicted insertion loss is similar but the values of the predicted and actual insertion loss sound pressure levels are not very similar. This is caused by two things. The poor actual performance of the enclosure is caused by the opening for the exhaust and the opening left for the cooling inlet. Application of the model based on a sealed enclosure to the practical case of an enclosure with openings enclosure is a "best guess" approach. The actual insertion loss will obviously be much less than the predicted insertion loss because the model is based on an ideal sealed environment. A more realistic model would include the effects of the openings, but this is material dependent and dependent on the size of the openings.

The optimal design code uses a noise spectrum calculated according to ISO specifications. This sound pressure level measurement includes the sound pressure level caused by the exhaust. This results in the optimal design code that predicts the material properties of an enclosure using the sound pressure level of the exhaust. However, it was suggested in Chapter 4 that the exhaust be handled outside the enclosure by an expansion chamber. An insertion loss model should be developed that will eliminate the exhaust noise to be more realistic and accurate. By developing a means to separate the exhaust sound pressure level from the rest of the noise spectrum, the optimization code will develop a better optimal design specifically for the noise caused by the generator and the engine without the exhaust noise.

The insertion loss model is a fair representation of the insertion loss. It is effective in the optimization code to predict the optimum material properties for the enclosure. With a heavy amount of engineering and design, an enclosure could be built that would reduce the radiated sound pressure level by approximately 15 dB. The amount of time and engineering money might not make it a commercially attractive project, but it can be accomplished.

5.1 Future work and considerations

This is just the beginning of the design for an acoustical hood of a generator. The results of the model worked well for the sealed aluminum test box. However, because of the openings that had to be left in the generator enclosure, the predictability of an actual enclosure was not very robust.. This is discussed in Chapter 3, where the performance of the wood enclosure is less than the predicted performance. More acoustical study should be investigated to include the degradation in the insertion loss due to the openings left in the enclosure. There is also a need to investigate the values of using ducts in non-sealed acoustical hoods.

An inlet duct, that allows the passage of cooling air through the enclosure is also a necessary area of investigation. The duct can be designed possibly for specific frequencies. The design of such a duct will also lend itself to two types of noise control. First, the duct will provide some passive acoustical control. Secondly, this would be a place to add active noise

control. Active control would allow the specific targeting of frequencies that need to be attenuated more than others.

Fair results can be achieved using just an optimal enclosure design, but the exhaust still poses a significant obstacle in designing an effective enclosure. Studies could be conducted to determine the contribution of the exhaust to the overall radiated sound pressure level. This might also reveal a procedure to separate the exhaust noise from the “other” engine noises and the generator noise. It is proposed that a tunable expansion chamber be designed that will be attached to the outside of the enclosure. The ability to tune the expansion chamber will allow a more specific design depending on the generator noise spectrum. Placing the muffler on the outside of the enclosure will eliminate the exhaust as a source of heat inside the enclosure.

One area of passive acoustical control that was not even presented here, is the use of acoustical liners or foam. This would require extensive model development to predict the performance of an acoustical hood lined with foam. Once an adequate model is developed it could be incorporated into the optimization program.

A more thorough heat transfer analysis is necessary in this study. Also, the heat transfer model presented here is completely theoretical. Obtaining complete, actual data was unavailable due to mechanical difficulties with the generator.

The model used here is a good predictor of the insertion loss for a sealed enclosure. Work with the aluminum test boxes discussed in Chapter 3 proved this. With the insertion loss model working, the optimization code works very well to determine the optimal material properties and panel thickness for the enclosure. The iteration process takes about 25 to 30 iterations before it settles on the optimized material values. The optimization program can be set to be sensitive toward the overall sound pressure level or more toward the weight of the enclosure. The optimized material values will also depend on the noise spectrum given to the optimization code. This allows this study to be very unique for future applications. The test performed with the wood enclosure proved that openings in the enclosure will degrade the performance and it is necessary to develop a process to predict the effects of such openings in an enclosure. However for the optimization process, the sealed enclosure model is a reasonable predictor of insertion loss. It accurately predicts the frequency at which the effects of the panel modes can be seen in the insertion loss. It also determines the effects of the source to panel distance on the insertion loss for the higher frequencies. Only the theoretical heat transfer requirements are discussed, but actual data collected using the wood enclosure suggests that the thermal issues should not pose a serious problem to the design of an enclosure.

The generator does not exceed its operating boundaries determined by Briggs and Stratton while enclosed and operating under a load. Even with a wood enclosure, and the exhaust of the generator vented directly to the outside of the enclosure, a 7db reduction was achieved in the overall radiated sound pressure level. With further study into the design of an expansion chamber to be attached to the enclosure and a deeper study into the thermal requirements, a reduction of 15 to 20 dB in the radiated sound pressure level seems to be possible. The enclosure might not be economically a commercial product, but it would be worth the production and engineering costs in noise controlled environments.

APPENDIX

Appendix I

Calculation of Sound power Level for the Test Generator

The International Standards Organization (ISO) outlines detailed procedures to calculate the overall sound pressure and sound power levels of noise sources. There are different standards for measurements in an anechoic, reverberant, and free fields. The following calculations are for a noise source in a free field environment according to ISO standard 1344.

A test surface had to be determined according to the size of the noise source. The determination of radius, r , of the hemispherical measurement surface was calculated according to ISO specifications. The specifications require the radius to be equal, or greater than twice the minimal dimension, d_0 , and not less than 1 meter. The following figure is a representation of the generator.

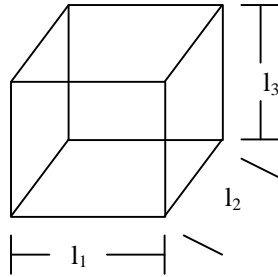


Figure A1: Dimensions of the generator

where: l_1 , l_2 , and l_3 are the length, width and height of the noise source respectively. For the test generator used in this investigation the measurements are:

$l_1 = .432$ m., $l_2 = .667$ m and $l_3 = .476$ m

The minimal dimension was calculated by:

$$d_0 = \sqrt{\left(\frac{l_1}{2}\right)^2 + \left(\frac{l_2}{2}\right)^2 + (l_3)^2} \quad (\text{A1})$$

The reason the l_3 term is not halved under the radical is because the noise source is located on one reflecting surface. Subsequently, $d_0 = .62$ m. It was decided that since the nominal dimension was less than 1 meter, the radius of the measurement would be approximately three times this dimension in order to make the radius of the test surface exactly equal to two meters.

Microphones were placed at the above ten locations to measure the sound pressure level.

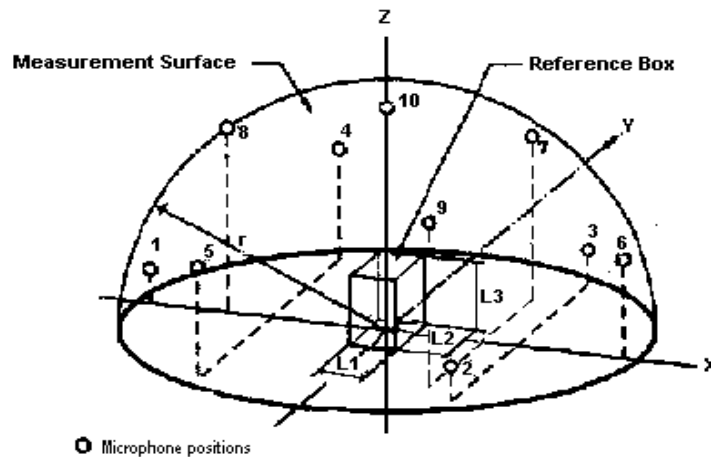


Figure A2: Test Measurement Surface

Table A1 lists the x, y, z coordinates of the ten microphone positions used in the test measurement.

Table A1: X, Y, Z coordinates of test surface

Microphone Position	X (m)	Y (m)	Z (m)
1	-1.98	0	.3
2	1	-1.72	.3
3	1	1.72	.3
4	-.9	1.54	.9
5	-.9	-1.54	.9
6	7.78	0	.9
7	-.66	1.14	1.5
8	-1.32	0	1.5
9	.66	-1.14	1.5
10	0	0	2

Figure A3 is the measured sound pressure level according to ISO specifications.

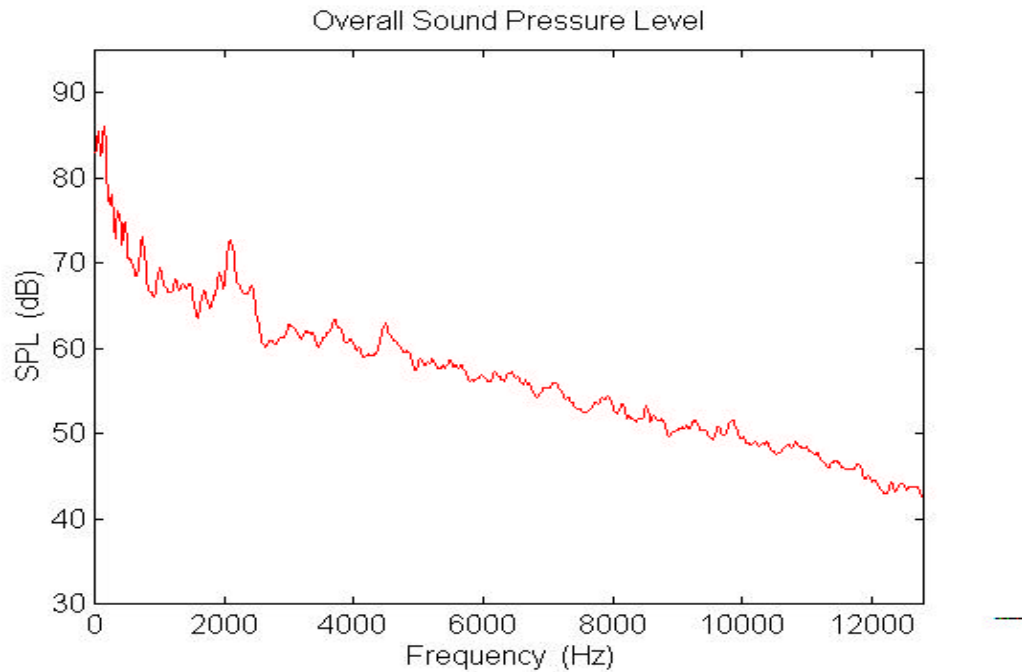


Figure A3: Measured Generator Overall Sound Pressure Level

This is a broad band noise spectrum of the test generator used as a reference for the investigation. Most of the noise is low frequency with a concentration of sound pressure level around 200 Hz and 2000 Hz. Knowing the sound pressure level of the source, the sound power level can be calculated. The sound power levels were grouped into their respective third octave bands and an overall sound power level was calculated. Figure A4 shows the sound power levels for the third octave bands.

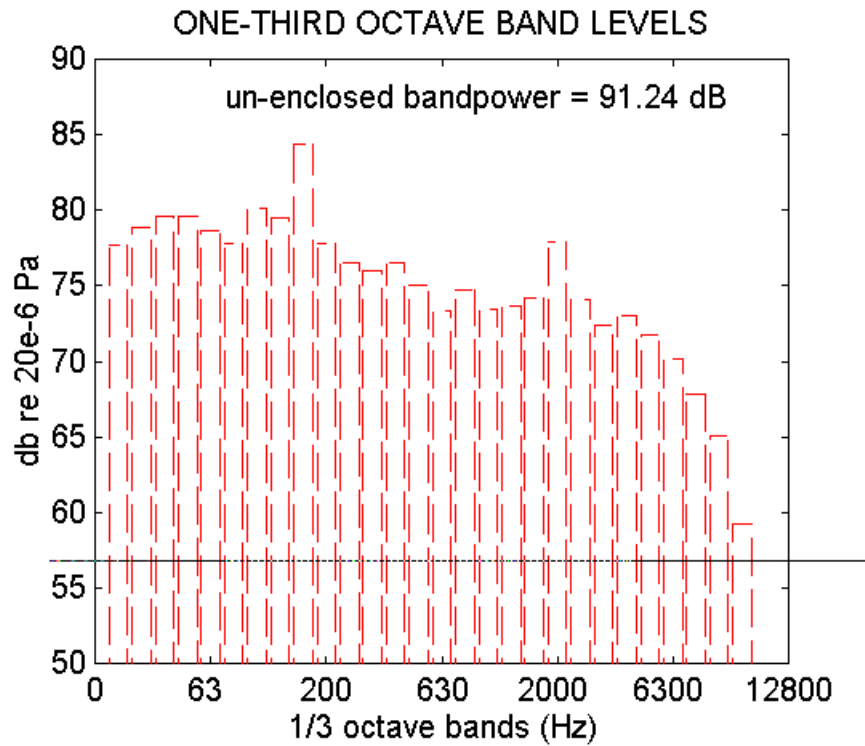


Figure A 4: Measured generator sound power level in 1/3 band octaves

Sound pressure and sound power do not have much relevance to most humans, so a scale, measured in sones, was developed to calculate the loudness of a noise source. This measures how 'loud' a person would perceive the noise. Figure A5 shows the overall loudness is measured to be 83.46 sones.

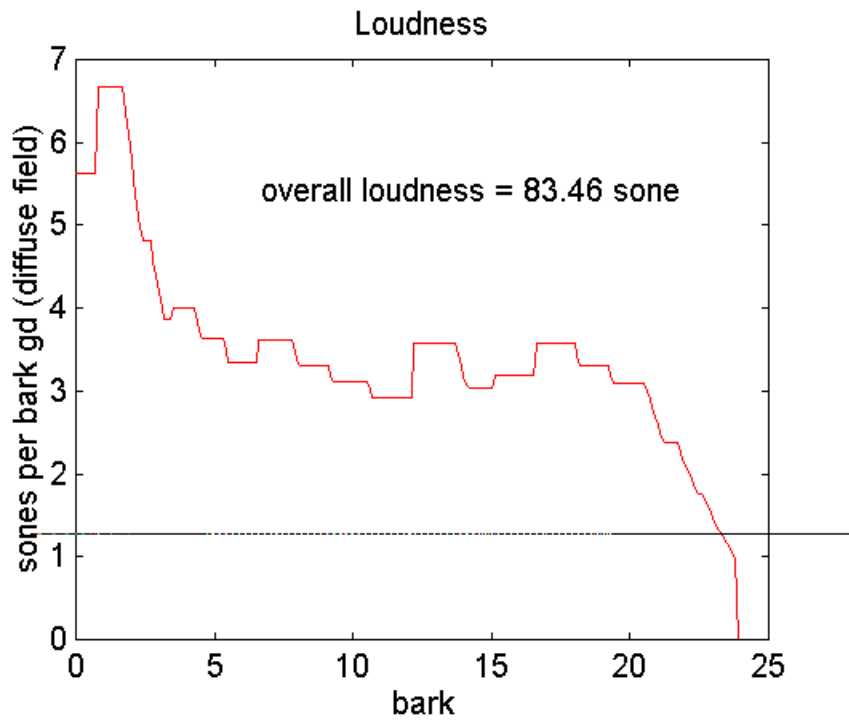


Figure A5: Measure Loudness of the Generator (based on Zweiker's methods)

Appendix II

Optimization Code

```
% This is the m file named gui.m
% This file creates the GUI for the enclosure optimization

close all
clear all
figure( ...
    'Name','Optimization GUI for Generator Enclosure', ...
    'NumberTitle','off')
SETFSIZE(785,605);

% colors: yellow, magenta, cyan, red, green, blue, white, black

% frame that contains all groups
frame_opt = uicontrol(gcf,...
    'Style','frame','BackgroundColor','blue',...
    'Position', [5 5 780 600]);

% frame that contains material properties
frame_prop = uicontrol(gcf,...
    'Style','frame','BackgroundColor','cyan',...
    'Position', [15 275 200 250]);

% frame that contains enclosure size
frame_enc = uicontrol(gcf,...
    'Style','frame','BackgroundColor','cyan',...
    'Position', [290 250 200 275]);

% frame that contains weighting values
frame_val = uicontrol(gcf,...
    'Style','frame','BackgroundColor','cyan',...
    'Position', [565 325 200 200]);

% frame at bottom
frame_cost = uicontrol(gcf,...
    'Style','frame','BackgroundColor','cyan',...
    'Position', [15 10 200 100]);

% Text control that titles thegui
txt_title=uicontrol(gcf,...
'Style','Text','BackgroundColor','white',...
'String','Initial Search Values',...
'Position',[215 550 350 25]);
```



```

%Text control that titles the material properties
txt_title=icontrol(gcf,...
'Style','Text','BackgroundColor','white',...
'String','Initial Material Properties',...
'Position',[20 495 190 25]);

```

```

%Text control that titles the enclosure dimensions
txt_title=icontrol(gcf,...
'Style','Text','BackgroundColor','white',...
'String','Set Maximum Enclosure Dimensions (in)',...
'Position',[295 475 190 40]);

```

```

%Text control that titles the Weighting Values
txt_title=icontrol(gcf,...
'Style','Text','BackgroundColor','white',...
'String','Weighting Values',...
'Position',[570 495 190 25]);

```

```

%Text control that titles the Estimated Cost
txt_title=icontrol(gcf,...
'Style','Text','BackgroundColor','white',...
'String','Estimated cost/area ($f)',...
'Position',[20 70 190 25]);

```

```

% *****%

```

```

%Material Box
%-----%
% Density
%Text control for density
txt_title=icontrol(gcf,...
'Style','Text','BackgroundColor','white',...
'String','Material Density (kg/m^3)',...
'Position',[20 450 130 35]);

```

```

%Editable text for entry of Density
DEN= uicontrol(gcf, 'Style','edit',...
'String','2700',...
'BackgroundColor','white','Position',[ 160 450 50 35]);

```

```

%-----%
% Internal Damping

```

```

%Text control for Internal DampingCoeff.
txt_title=icontrol(gcf,...
'Style','Text','BackgroundColor','white',...
'String','Internal Damping Coeff.',...
'Position',[20 400 130 35]);

```

```
%Editable text for entry of Internal Damping
ID= uicontrol(gcf, 'Style','edit',...
'String','.001',...
'BackgroundColor','white','Position',[ 160 400 50 35]);
```

```
%-----%
% Young's Modulus
```

```
%Text control for Young's Modulus
txt_title=icontrol(gcf,...
'Style','Text','BackgroundColor','white',...
'String','Young`s Modulus (N/m^2)',...
'Position',[20 350 125 35]);
```

```
%Editable text for entry of Young's Modulus
YM= uicontrol(gcf, 'Style','edit',...
'String','7.16e10',...
'BackgroundColor','white','Position',[ 155 350 55 35]);
```

```
%-----%
% Poisson`s Ratio
```

```
%Text control forPoisson`s Ratio
txt_title=icontrol(gcf,...
'Style','Text','BackgroundColor','white',...
'String','Poisson`s Ratio',...
'Position',[20 300 130 35]);
```

```
%Editable text for entry ofPoisson`s Ratio
PR= uicontrol(gcf, 'Style','edit',...
'String','.34',...
'BackgroundColor','white','Position',[ 160 300 50 35]);
```

```
% *****%
```

```
%Enclosure Size Box
%-----%
```

```
% height
%Text control for height
txt_title=icontrol(gcf,...
'Style','Text','BackgroundColor','white',...
'String','height (18.75 min. )',...
'Position',[295 425 130 35]);
```

```
%Editable text for entry of height
HGT= uicontrol(gcf, 'Style','edit',...
'String','18.75',...
'BackgroundColor','white','Position',[ 435 425 50 35]);
```

```

%-----%
% length
% Text control for length
txt_title=uicontrol(gcf,...
'Style','Text','BackgroundColor','white',...
'String','length (26.25 min. )',...
'Position',[295 375 130 35]);

%Editable text for entry of length
LGTH= uicontrol(gcf, 'Style','edit',...
'String','26.25',...
'BackgroundColor','white','Position',[ 435 375 50 35]);

%-----%
% width
% Text control for width
txt_title=uicontrol(gcf,...
'Style','Text','BackgroundColor','white',...
'String','width (17 min. )',...
'Position',[295 325 130 35]);

%Editable text for entry of width
WDTH= uicontrol(gcf, 'Style','edit',...
'String','17',...
'BackgroundColor','white','Position',[ 435 325 50 35]);

%-----%
% Panel Thickness
% Text control for Panel Thickness
txt_title=uicontrol(gcf,...
'Style','Text','BackgroundColor','white',...
'String','Panel Thickness',...
'Position',[295 275 130 35]);

%Editable text for entry of Panel Thickness
PT= uicontrol(gcf, 'Style','edit',...
'String','.125',...
'BackgroundColor','white','Position',[ 435 275 50 35]);

% *****%
% Weighting Box
%-----%
% Insertion Loss weight
% Text control for Insertion Loss weight
txt_title=uicontrol(gcf,...
'Style','Text','BackgroundColor','white',...
'String','Insertion Loss weight (1-10)',...
'Position',[570 450 130 35]);

%Editable text for entry of Insertion Loss weight

```

```

WIL= uicontrol(gcf, 'Style','edit',...
'String','1',...
'BackgroundColor','white','Position',[ 710 450 50 35]);

%-----%
% Enclosure weight

%Text control for Enclosure weight
txt_title=uicontrol(gcf,...
'Style','Text','BackgroundColor','white',...
'String','Enclosure weight (1-10)',...
'Position',[570 400 130 35]);

%Editable text for entry of Enclosure weight
WS= uicontrol(gcf, 'Style','edit',...
'String','1',...
'BackgroundColor','white','Position',[ 710 400 50 35]);

%-----%
% Cost weight

%Text control for Cost weight
txt_title=uicontrol(gcf,...
'Style','Text','BackgroundColor','white',...
'String','Cost weight (1-10)',...
'Position',[570 350 130 35]);

%Editable text for entry of Cost weight
WC= uicontrol(gcf, 'Style','edit',...
'String','1',...
'BackgroundColor','white','Position',[ 710 350 50 35]);

% *****%
%Cost Estimation Box
%-----%
% frame around entry box
frame_prop = uicontrol(gcf,...
'Style','frame','BackgroundColor','black',...
'Position', [80 30 70 35]);
%Editable text for Cost Estimation Box
WCE= uicontrol(gcf, 'Style','edit',...
'String','100',...
'BackgroundColor','white','Position',[ 85 35 60 25]);
%-----%

% *****%
%Create Push Button start

```

```

% frame that contains material properties
frame_s = uicontrol(gcf,...
    'Style','text','BackgroundColor','white',...
    'String','Start the Optimization Program',...
    'Position', [578 50 160 35]);

% frame around start button
frame_as = uicontrol(gcf,...
    'Style','frame','BackgroundColor','black',...
    'Position', [620 10 70 35]);

pbstart = uicontrol(gcf,'Style','push',...
    'BackgroundColor','white','Position',[625 15 60 25],...
    'String','Start','Callback','init');

% *****%
% source to panel distance box

% frame that sets source to panel distance
frame_prop = uicontrol(gcf,...
    'Style','frame','BackgroundColor','cyan',...
    'Position', [15 115 200 135]);

% Text control that titles the source to panel distance
txt_title= uicontrol(gcf,...
    'Style','Text','BackgroundColor','white',...
    'String','Set the Source-to-panel Distance (in)',...
    'Position',[20 210 190 35]);

% Text control that titles the source to panel distance width
txt_title= uicontrol(gcf,...
    'Style','Text','BackgroundColor','white',...
    'String','STP Dist. width',...
    'Position',[20 180 140 25]);

% Editable text for entry of STP width
DWDTH= uicontrol(gcf, 'Style','edit',...
    'String','8.5',...
    'BackgroundColor','white','Position',[165 180 40 25]);

% Text control that titles the source to panel distance length
txt_title= uicontrol(gcf,...
    'Style','Text','BackgroundColor','white',...
    'String','STP Dist. length',...
    'Position',[20 150 140 25]);

% Editable text for entry of STP length
DLGTH= uicontrol(gcf, 'Style','edit',...
    'String','13.125',...

```

```

'BackgroundColor','white','Position',[165 150 40 25]);

%Text control that titles the source to panel distance height
txt_title=icontrol(gcf,...
'Style','Text','BackgroundColor','white',...
'String','STP Dist. height',...
'Position',[20 120 140 25]);

%Editable text for entry of STP height
DHGT=icontrol(gcf, 'Style','edit',...
'String','9.375',...
'BackgroundColor','white','Position',[165 120 40 25]);

%-----%
%Settings for output box

% frame that contains output
frame_out = uicontrol(gcf,...
    'Style','frame','BackgroundColor','cyan',...
    'Position', [290 10 225 230]);

%Text control for Panel Thickness
txt_title=icontrol(gcf,...
'Style','Text','BackgroundColor','white',...
'String','Panel Thickness (m)',...
'Position',[295 15 130 30]);

%Text control for Young's Modulus
txt_title=icontrol(gcf,...
'Style','Text','BackgroundColor','white',...
'String','Weight (kg)',...
'Position',[295 50 130 35]);

%Text control for Young's Modulus
%txt_title=icontrol(gcf,...
%'Style','Text','BackgroundColor','white',...
%'String','Young`s Modulus (N/m^2)',...
%'Position',[295 50 130 35]);

%Text control for Internal DampingCoeff.
txt_title=icontrol(gcf,...
'Style','Text','BackgroundColor','white',...
'String','Internal Damping Coeff.',...
'Position',[295 90 130 35]);

%Text control forPoisson`s Ratio
txt_title=icontrol(gcf,...
'Style','Text','BackgroundColor','white',...

```

```
'String','Poisson`s Ratio',...  
'Position',[295 130 130 25]);
```

```
% Text control for density  
txt_title=icontrol(gcf,...  
'Style','Text','BackgroundColor','white',...  
'String','Material Density (kg/m^3)',...  
'Position',[295 160 130 35]);
```

```
% Text control that titles the optimized material properties  
txt_title=icontrol(gcf,...  
'Style','Text','BackgroundColor','white',...  
'String','Optimized Material Properties',...  
'Position',[295 200 215 35]);
```

```
%-----%
```

```
clear ans frame_as frame_cost frame_enc frame_prop...  
frame_s frame_val pbstart txt_title frame_opt frame_out
```

```

% This m file is called init.m
% This program reads the values entered into the GUI
%
%
clear a b c mu E neta rho_mat h c_air rho_c
%-----

% Properties of air

rho_c=406;
c_air=343; %m/s

%-----%
% Error Messages

if str2num(get(DEN,'String'))<=0
    error('Density Value must be positive')
end

if str2num(get(ID,'String'))<=0
    error('Internal Damping Ratio Value must be positive')
end

if str2num(get(YM,'String')) <= 0
    error('Young`s Modulus Value must be positive')
end

if str2num(get(PR,'String')) <= 0
    error('Poisson`s Ratio Value must be positive')
end

if str2num(get(HGT,'String')) < 18.75
    error('Height Value below minimum');
end

if str2num(get(LGTH,'String')) < 26.25
    error('Length Value below minimum')
end

if str2num(get(WDTH,'String')) < 17
    error('Width Value below minimum')
end

if str2num(get(PT,'String')) < .03125
    error('Panel Thickness Value must be greater than .03125')
end

if str2num(get(DWDTH,'String')) < 8.5
    error('Source-to-panel distance (width) must be greater than 8.5')
end

```



```

if str2num(get(DHGT,'String')) < 9.375
    error('Source-to-panel distance (height) must be greater than 9.375')
end

if str2num(get(DLGTH,'String')) < 13.125
    error('Source-to-panel distance (length) must be greater than 13.125')
end

%-----%

rho_mat=str2num(get(DEN,'String'));

neta =str2num(get(ID,'String'));

mu=str2num(get(PR,'String'));

E=str2num(get(YM,'String'));
%-----%

% The initial dimensions of the enclosure
% a is the height, b is the width and c is the length

maximum_a=str2num(get(HGT,'String'))*.0254; %in*m/in (height);

maximum_b=str2num(get(WDTH,'String'))*.0254; %in*m/in (width);

maximum_c=str2num(get(LGTH,'String'))*.0254; %in*m/in (length);

%-----%
% Get the source to panel settings
da=str2num(get(DHGT,'String'))*.0254; %in*m/in (height);
db=str2num(get(DWDTH,'String'))*.0254; %in*m/in (width);
dc=str2num(get(DLGTH,'String'))*.0254; %in*m/in (length);

%-----%
% calculate the panel dimensions
a=(9.375*.0254)+da;
b=2*db;
c=2*dc;

%-----%
% Thickness of the panel.

h=str2num(get(PT,'String'))*.0254; %in*m/in

%-----%

```

```

%Calculate mass density
m=rho_mat*h;

weight_cost = str2num(getWC,'String');
weight_enclosure = str2num(getWS,'String');
weight_il = str2num(getWIL,'String');
cost_per_area = str2num(getWCE,'String');

%-----%
clear DEN DHGT DLGTH DWDTH HGT ID LGTH PR PT WC WCE WPTH WIL WS YM

%Run calculation files
load generato
min_max;

run3file;

%clear PT YM PR HGT LGTH WPTH ID DEN WC WIL WCE WS DHGT DLGTH DWDTH

```

```

% This is the m file named run_file.m
% This file runs the satellite files that calculates the optimum material properties

% *****
% Load the generator noise spectrum

load generato;          % This returns the vector total_spl

% Run minimum and maximum file that sets the respective
% values for the material properties

min_max;

step_mat = 50;
step_h = 3.5455e-4;

rho_mat = min_rho_mat - step_mat;
h = min_h - step_h;
org_h = min_h;
count = 0;

for mc = 1:66
    rho_mat = rho_mat + step_mat;

    for hc = 1:66;
        h = h + step_h;

        panel;
        predict;
        perform;

        count = count + 1;

        hp(hc) = h;
        perf(mc, hc) = new_perf_index;
        spl(mc, hc) = over_all_spl;

        big_one(count, :) = [rho_mat h new_perf_index over_all_spl];
    end
    rho(mc) = rho_mat;
    h = org_h;
end

[minimum_perf location_perf] = min(big_one(:, 3));
[minimum_spl location_spl] = min(big_one(:, 4));

h = big_one(location_perf, 2);
rho_mat = big_one(location_perf, 1);

save vector3 perf spl hp rho big_one;

```

panelil;
predict;
perform;

moregui;
show;

```
% This is the m file called minmax.m
% This file sets the limits for the material properties
% (panel thickness, material density, internal damping,
% young's modulus and poissons ratio)
```

```
max_rho_mat=4500;    %max material density (kg/m^3)
min_rho_mat = 600;  %min material density (kg/m^3)
max_neta=.01;       %max internal damping coeff
min_neta = .0016;   %min internal damping coeff
max_h=.00635;       %max panel thickness (m)
min_h = .0016;      %min panel thickness (m)
max_E=10e10;        %max Youngs modulus
min_E = 5e5;        %min Youngs modulus
max_mu=.4;          %max poissons ratio
min_mu = .3;        %min poissons ratio
```

```

% This is the m file called panel/m
% This file calculates the insertion loss of a given box

% Make the frequency vector

freq=[0:16:12800];
freq(1) = 1;

% Bulk modulus of the material
D=(E*(h^3))/(12*(1-mu^2));

% Distance from noise source, assuming the center of the
% equipment is the noise center for side a

d=da;

omega = 2.*pi.*freq;           %rad/sec
k=omega./c_air;                %rad/m
kd=k.*d;                       %rad
D=(E*(h^3))/(12*(1-mu^2));     %N.m

% Oldham's equation for insertion loss of a close panel with clamped boundary conditions

Dstar = D * (1 + (j * neta));
K = 1.35 ./ (3.86 * Dstar * ((129.6/b^4) + (78.4/(c^2 * b^2)) + (129.6/c^4)) - (omega.^2 * rho_mat * h));
IL_top = 10 .* log10((cos(kd) + (pi^2 ./ (4 .* K .* omega .* rho_c)) .* sin(kd)).^2);

% This controls the depths of the nulls of the insertion loss
% Because of the equation, the nulls become infinite depending on the
% sampling of the frequency

Pmax = IL_top(1);
for ZZ = 2:length(freq)
    if IL_top(ZZ) > IL_top(ZZ-1)
        Pmax = IL_top(ZZ);
    end

    if IL_top(ZZ) < Pmax - 20
        IL_top(ZZ) = Pmax - 20;
    end
end

% The next panel

d = dc;

```

%Oldham's equation for insertion loss of a close panel with clamped boundary conditions

```
Dstar = D * (1 + (j * neta));  
K = 1.35 ./ (3.86 * Dstar * ((129.6/a^4) + (78.4/(a^2 * b^2)) + (129.6/b^4)) - (omega.^2 * rho_mat * h));  
IL_side_b = 10 .* log10((cos(kd) + (pi^2 ./ (4 .* K .* omega .* rho_c)) .* sin(kd)).^2);
```

%This controls the depths of the nulls of the insertion loss
%Because of the equation, the nulls become infinite depending on the
%sampling of the frequency

```
Pmax = IL_side_b(1);  
for ZZ = 2:length(freq)  
    if IL_side_b(ZZ) > IL_side_b(ZZ-1)  
        Pmax = IL_side_b(ZZ);  
    end  
  
    if IL_side_b(ZZ) < Pmax - 20  
        IL_side_b(ZZ) = Pmax - 20;  
    end  
end
```

%next panel

d = db;

%Oldham's equation for insertion loss of a close panel with clamped boundary conditions

```
Dstar = D * (1 + (j * neta));  
K = 1.35 ./ (3.86 * Dstar * ((129.6/a^4) + (78.4/(a^2 * c^2)) + (129.6/c^4)) - (omega.^2 * rho_mat * h));  
IL_side_c = 10 .* log10((cos(kd) + (pi^2 ./ (4 .* K .* omega .* rho_c)) .* sin(kd)).^2);
```

%This controls the depths of the nulls of the insertion loss
%Because of the equation, the nulls become infinite depending on the
%sampling of the frequency

```
Pmax = IL_side_c(1);  
for ZZ = 2:length(freq)  
    if IL_side_c(ZZ) > IL_side_c(ZZ-1)  
        Pmax = IL_side_c(ZZ);  
    end  
  
    if IL_side_c(ZZ) < Pmax - 20  
        IL_side_c(ZZ) = Pmax - 20;  
    end  
end
```

```
il_band;           %Calculates the insertion loss across the bandwidth
```

```
predict;          %Call the mfile to predict the spl spectrum of the enclosure
```



```

% This m file is called il_band
% This file calculates the insertion loss over the band width

for this=1:length(freq)
    sum(this)=10^(IL_top(this)/10)+10^(IL_side_b(this)/10)+...
              10^(IL_side_b(this)/10)+10^(IL_side_c(this)/10)+...
              10^(IL_side_c(this)/10);
end
% Average the insertion loss for the five sides of the panel
for this=1:length(freq)
    il_band_total(this)=10*log10(sum(this)/5);
end

save iltot il_band_total

```

```
% This program is \called pattern
% This program does the pattern search
```

```
flag2 = 0;
```

```
while flag2 == 0
```

```
%-----
% These if loops limit the variables to their respective minimums
% and maximums
```

```
    panelil;
    predict;
    perform;
    old_perf_index = new_perf_index;
```

```
    rho_mat = rho_mat + step_mat;
    if rho_mat >= max_rho_mat
        rho_mat = max_rho_mat;
    end
    if rho_mat < min_rho_mat;
        rho_mat = min_rho_mat;
    end
```

```
    h = h + step_h;
    if h >= max_h
        h = max_h;
    end
    if h < min_h
        h = min_h;
    end
```

```
%-----
% Calculate the insertion loss of the enclosure
```

```
    panelil;
    predict;
    perform;
```

```
if old_perf_index < new_perf_index;
    flag2 = 1;
    break_flag = break_flag + 1;
end % if
```

```

if flag2 == 0
    count = count + 1;
    temp_vbl(count, 1) =rho_mat;
    temp_vbl(count, 2) = h;

    big_perf(count)=new_perf_index;
    big_il(count)=over_all_spl;
    big_h(count)=h;
    big_rho(count) =rho_mat;
    big_step_h(count) =step_h;
    big_step_mat(count) =step_mat;

end % if

flag2

end % while

rho_mat = temp_vbl(count, 1);
h = temp_vbl(count, 2);

clear old_perf_indexnew_perf_index

```

```
% This m file is called spl_oa.m  
% This file calculated the predicted SPL of the enclosure
```

```
clear sum over_all_spl
```

```
sum=0;  
orig = 0;
```

```
for this=1:length(freq)
```

```
    sum=sum+10^(real(i_l_band_total(this))/10);  
    orig = orig + 10^(total_spl(this)/10);
```

```
end
```

```
over_all_spl=10*log10(sum);  
orig_total = 10*log10(orig);
```

```
% This is the m file calledperfore.m
% This file is the performance index calculation

clear new_perf_index

new_perf_index = (weight_il*over_all_spl) + (weight_enclosure);
```

```
% This is the m file called predict.m
% This file calculates the predicted spl spectrum of the generator
% with the enclosure
```

```
predicted_spl = (total_spl) - real(il_band_total);
```

```
for ZZ = 1:length(freq)
    if predicted_spl(ZZ) < 0
        predicted_spl(ZZ) = 0;
    end
end
```

```
end
```

```
spl_oa;
```

```
acw;
```

```

% This is the mfile called moregui.m
% This file fills in the optimized values into thegui

% Text control for Panel Thickness output
txt_title=icontrol(gcf,...
'Style','Text','BackgroundColor','white',...
'String','h,...
'Position',[430 15 75 30]);

% Text control for weight
txt_title=icontrol(gcf,...
'Style','Text','BackgroundColor','white',...
'String','weight,...
'Position',[430 50 75 35]);

% Text control for Young's Modulus
txt_title=icontrol(gcf,...
'Style','Text','BackgroundColor','white',...
'String','E,...
'Position',[430 50 75 35]);

% Text control for Internal DampingCoeff.
txt_title=icontrol(gcf,...
'Style','Text','BackgroundColor','white',...
'String','neta,...
'Position',[430 90 75 35]);

% Text control forPoisson`s Ratio
txt_title=icontrol(gcf,...
'Style','Text','BackgroundColor','white',...
'String','mu,...
'Position',[430 130 75 25]);

% Text control for density
txt_title=icontrol(gcf,...
'Style','Text','BackgroundColor','white',...
'String','rho_mat,...
'Position',[430 160 75 35]);

```

```
% This file is called acw.m
% This file calculates the surface of the area and weight of the enclosure

area=(b*c)+(2*(a*b))+(2*(b*c));

weight=area*h*rho_mat;

% cost=area*cost_per_area;
```



```

% This m file is called show.m
% This file plots the stuff from pattern

figure
plot(big_perf)
title('Performance index')

figure
plot(big_il)
title('Calculated Total SPL')

figure
plot(big_h)
title('Panel thicknesses')

figure
plot(big_step_h)
axis([0 40 -.00001 .00001])
title('Step sizes of Panel Thicknesses')

figure
plot(big_rho)
title('Material Densities')

figure
plot(big_step_mat)
title('Step sizes of Material Densities')

figure
semilogx(freq,total_spl)
hold on
plot(freq,predicted_spl,'r--')
hold off
axis([0 12800 0 100])
title('Actual vs Predicted SPL of Generator')
legend('Actual','Predicted')
datau = ['Total SPL = ' num2str(over_all_spl) ' dB'];
gtext(datau)

```

Bibliography

1. L.L. Beranek and I. L. Ver, 1992 *Noise and Vibration Control Engineering* New York, John Wiley and Sons.
2. F. Fahy, 1989, *Sound and Structural Vibration* San Diego, Ca. Academic Press Limited.
3. L.E. Kinsler and A.R. Frey, 1982 *Fundamentals of Acoustics*, New York, John Wiley and Sons.
4. M. Rettinger, 1973, *Acoustic Design and Noise Control*, Chemical Publishing Company, New York.
5. D.J. Oldham and S.N. Hilarby, 1991. "The Acoustical Performance of Small Close Fitting Enclosures, Part 1; Theoretical Models" *Journal of Sound and Vibration*, vol. 150 pp. 261-81.
6. D.J. Oldham and S.N. Hilarby, 1991. "The Acoustical Performance of Small Close Fitting Enclosures, Part 2; Experimental Investigation" *Journal of Sound and Vibration*, vol. 150 pp. 283-300.
7. K.P. Bryne, H.M. Fischer and H.V. Fuchs, 1988. "Sealed, Close Fitting, Machine Mounted Acoustic Enclosures with Predictable Performance" *Noise Control Engineering Journal*, vol. 31, no. 1, pp. 7-14.
8. R.Y. Vinokur, July, 1996. "Evaluating Sound Transmission Effect in Multi-Layer Partitions", *Sound and Vibration*".
9. E.D. Eason and R.G. Fenton, February, 1974. "A Comparison of Numerical Optimization Methods for Engineering Design" *Journal of Engineering for Industry* pp. 196-200.
10. J. Roberts, September, 1990. "The Principle of Noise Control with Enclosures" *Journal of Electrical and Electronic Engineering, Australia* vol. 10, no. 3, pp.151-155.
11. ISO 3740-1980, *Acoustics - Determination of Sound Power Levels of Noise Sources - Guidelines for the use of basic Standards and Preparations of noise test code*, International Standards Organization.
12. Michael Rettinger, 1973 *Acoustic Design and Noise Control*, Chemical Publishing Co., Inc., New York. pp. 129-140.
13. James N. Siddall, 1982 *Optimal Engineering Design; Principles and Applications*, Marcel Dekker, Inc., New York, chapters 2 - 8.

14. E. Buckingham, 1924. "Theory and Interpretation of Experiments on the Transmission of Sound through Partition Walls", *Sci. Papers Natn. Bur. Standards* vol. 20, p.193.
15. L.L. Beranek and G.A. Work, 1949. "Sound Transmission Through Multiple Structures Containing Flexible Blankets" *Journal of the Acoustical Society of America* vol.7, p.419.
16. Malcolm J. Crocker, 1994. "A Systems Approach to the Transmission of Sound and Vibration Through Structures", *Noise-Con 94*, pp. 525 - 533.
17. London, A., 1950. "Transmission of Reverberant Sound through Single Wall" *Journal of the Acoustical Society of America* vol. 22, p. 270 - 279.
18. Jackson, R.S., 1962. , "The Performance of Acoustic Hoods at Low Frequencies" *Acoustica*, vol. 12, pp.139 - 152.
19. Jackson, R.S., 1966. "Some Aspects of Acoustic Hoods" *Journal of Sound and Vibration*, vol. 3, pp. 82 - 94.
20. Junger, M.C., 1970. "Sound Through an Elastic Enclosure Acoustically Coupled to a Noise Source". *ASME Paper No. 70 - WA/DE - 12*
21. Walker, A.W., 1971. "Acoustic Materials for Absorption" *Conference on Noise and Vibration Control for Industries* pp. 7.1 - 7.4.
22. Bolton, J.S., Green,E.R., 1993. "Normal Incidence Sound Transmission through Double Panel Systems with Relatively Stiff, Partially Reticulated Polyurethane Foam" *Applied Acoustics*, vol. 39, pp. 23 - 51.
23. Maa, Dah-You, 1987. 'Microperforated-Panel Wide Band Absorbers' *Noise Control Engineering Journal* vol 29, no. 3, pp. 77 - 85.
24. Jinko, Lee, Sweenson, G.W., 1992 "Compact Sound Absorbers for Low Frequencies" *Noise Control Engineering Journal* vol. 3, no. 3, pp. 109 - 117.
25. Mumaw, James, 1996. "A comparison of Analytical Models and Experimental Results in a Non - Rigid Walled Enclosure", Masters Thesis in Mechanical Engineering at Virginia Tech.

Vita

Joe Blanks was born in South Boston, Virginia on January 21, 1972. Upon graduation from Cheyenne Central High School in Cheyenne, Wyoming in May 1990, he began his collegiate career at Virginia Military Institute. He graduated from VMI with distinction with a bachelor's of science in Mechanical Engineering and a minor in mathematics. After his undergraduate endeavors he secured employment at J. A. Jones Construction in Charlotte, North Carolina as an "Office Engineer" in the energy division. Finding this work unchallenging, he accepted another job after only four months in Charlotte at Omni Construction in Bethesda, Maryland as a Junior Mechanical Coordinator. Then an opportunity to return to graduate school was presented to him in May 1995. With the feeling that the job at Omni, too was stagnant, he returned to school as a graduate student at Virginia Tech in the mechanical engineering department to pursue more interesting avenues. He graduated from Tech in January 1997 with a master's degree in mechanical engineering. From Tech, he began a new career with Raytheon E-Systems in Falls Church, Virginia designing electronic packaging chassis.

Joseph Blanks